C.P. No. 846

C.P. No. 846

MINISTRY OF AVIATION

AERONAUTICAL RESEARCH COUNCIL

CURRENT PAPERS

Low-speed Wind-tunnel Measurements of the Lift, Drag and Pitching Moment on Three Symmetrical Ogee-Wing Models and on a Symmetrical Slender Wing-body Model

by

D. A. Kirby, B.Sc. A.C G.I., D.I.C.

LONDON: HER MAJESTY'S STATIONERY OFFICE

1966

EIGHT SHILLINGS NET

U.D.C. No. 533.6.013.13 : 533.6.013.12 : 533.6.013.152 :
533.695.12 : 533.693.4

C.P. No.846

November 1963

LOW-SPEED WIND-TUNNEL MEASUREMENTS OF THE LIFT, DRAG AND PITCHING MOMENT ON THREE SYMMETRICAL OGEE-WING MODELS AND ON A SYMMETRICAL SLENDER WING-BODY MODEL

by

D. A. Kirby, B.Sc., A.C.G.I., D.I.C.

SUMMARY

Measurements have been made of the lift, drag and pitching moment of three ogee models and a wing-body model, all having a slenderness ratio (semispan/root chord) of 0.209. The associated surface flow patterns were also observed.

Although the models were symmetrical and did not represent strictly comparable fully optimised designs of possible layouts for a supersonic transport, some useful low-speed aerodynamic comparisons between the integrated or ogee models and the wing-body model were obtained. The results show:-

(i) very similar lift characteristics,

(ii) a slightly smaller drag for the wing body model,

(iii) better static longitudinal stability characteristics for the wing-body model, especially when the wing planform was not faired smoothly into the body.

Attempts to improve the longitudinal stability of one of the ogee wings, by minor planform modifications at the rear of the wing intended to reduce the forward movement of aerodynamic centre with incidence, were largely unsuccessful, but provided some useful data on the effect of trailing-edge shape. For the wing-body model, drooping the nose was a successful modification and it is suggested that a drooped nose version of the wing-body model (without any planform fillet) would have good static longitudinal stability.

Replaces R.A.E. Tech. Note No. Aero 2927 - A.R.C. 25709

CONTENTS

TABLES

ILLUSTRATIONS

1 INTRODUCTION

This Note gives the results of 4 ft × 3 ft low-speed tunnel tests made as part of a general experimental investigation of the characteristics of various layouts for supersonic transport aircraft intended to cruise at Mach numbers in the region of 2.0. These layouts have included some configurations where the body is completely integrated with the wing and the resulting planform is ogee in shape, and others where the combination of a wing and body is more easily identifiable. The investigations reported here were concerned with the flow properties and the static longitudinal characteristics of four symmetrical models, namely three wings with ogee planforms and integrated bodies and one wing-body combination.

For all four models the slenderness ratio s/c_o was 0.209 while the planform area ratio $p(= S/bc_o)$ was 0.430, 0.450 and 0.467 for the ogee wings, and 0.455 for the wing-body combination. Allied studies of the effects of lengthwise and spanwise camber on the longitudinal characteristics of the p = 0.450 ogee planform are reported elsewhere[1].

In addition to the measurements on the four basic models, some attempts to alleviate the forward movement of aerodynamic centre with increase of lift were made on the p = 0.430 ogee wing and on the wing-body combination. The nature of these modifications is described in section 2 and the results discussed in section 3.3. A simplified wing-body model was also tested to find the contributions of the body and the planform fillets to the stability of the complete model, and an analysis of these tests is presented in section 3.4.

Studies of the flow over and around these models were made using surface flow and smoke techniques to see if the changes in sweep-back along the leading-edge and/or the presence of a body destroyed the unified flow originally aimed at in these slender shapes. The results of these observations are discussed in section 3.1.

2 DETAILS OF MODELS AND TESTS

The main dimensions of all the models are given in Table 1. The p = 0.430 ogee planform was taken from a project study by Hawker Siddeley Aviation, whilst the other two (with p = 0.450 and 0.467) were designed by Dr. J. Weber of R.A.E. to give more gradual changes of sweep-back along the leading-edge (Fig.1). The cross sections of all three models were simplified versions of the firms proposed "integrated" layout (Table 1 and Fig.1).

The wing-body model (p = 0.455) was made to a planform and sections obtained from an early Bristol Aircraft design by shearing the cambered sections of that design to give a symmetrical model. The planform of the wing blended via a fillet into a narrow strake on each side of the body (Figs.2 and 3). A further model (p = 0.450) was made with a detachable body and without fillets or strakes in order to investigate their effects*. The planform of this model

* Since one model had fillets and strakes and the other had neither, the terms "with fillet" and "without fillet" will be used in referring to these models in the test and figures.

is compared with that of the p = 0.450 ogee in Fig.3. All the models were made of wood.

Measurements of the lift, drag and pitching moment of the models were made in the 4 ft × 3 ft low-speed tunnel during 1960, using the normal wire rig and overhead balance. Most of the tests were made at a tunnel speed of 200 ft/sec, but, because of model vibration, for the ogee models at incidence above 20° the speed was reduced to 100 ft/sec. The incidence range was from -4° to 26°. The Reynolds based on the overall model lengths and a speed of 200 ft/sec ranged between 2.6 and 2.9×10^{6}. Except for a few surface flow tests, the transition was left free.

Since the tests showed a forward movement of aerodynamic centre with increase of lift, methods of alleviating this mild "pitch-up" were sought. For the ogee models, the effect of providing extra non-linear lift at the rear was investigated by attaching brass plates to the lower surface of the p = 0.430 model to extend the planform; six shapes were tried (Table 2 and Fig.4(a)). On the wing-body model, a decrease in the lift on the forebody was attempted, both by simple linear droop at the nose and by a parabolic droop (Table 2 and Fig.4(b)).

Visualization of the flow over the upper surface of all the models was obtained using lampblack suspended in paraffin[2] at tunnel speeds of up to 180 ft/sec. Some extra observations of the flow above the wing-body models were made at 10 ft/sec using liquid titanium tetrachloride which fumes in moist air. The models were transferred from the wire rig to a rear sting mounting for both these flow tests.

The results of all the balance measurements are presented in Tables 3-7 and discussed in section 3. The tunnel constraint corrections applied to the balance measurements include the effect of model length calculated by the method of Ref.3. Since breakdown of the leading-edge vortices did not occur for the range of incidence tested, there was only a small wake blockage correction.

3 RESULTS AND DISCUSSION

3.1 Flow visualization

From very low incidences the surface flow patterns on the ogee wings showed the presence of the leading-edge vortices which dominate the flow over slender wings with sharp edges. These vortices were continuous for all the models over the whole range of incidence covered; differences between the wings being limited to variations in the positions of the primary vortex. The spanwise location of this vortex can be conveniently specified by using the point of inflexion in the flow lines which are produced in the upper surface flow patterns. Fig.19 shows such patterns for the three ogee wings at an incidence of 15°. At this incidence, at 50% root chord the spanwise positions of the primary vortex were as follows:-

p	0.430	0.450	0.467
y/s'	0.42	0.53	0.55

whilst for all three wings the secondary separation occurred at $y/s' \simeq 0.7$.

At lower incidences, up to about 5°, there were some signs of further flow separations inboard of the primary vortex attachment lines on the forward part of the wings. However, these were considered to be an effect of the low Reynolds number of the tests and were eliminated when a transition wire was fixed round the nose.

For the complete wing-body model the flow was more complex. At 5° of incidence the flow was still attached on the body with the wing leading-edge separation starting in the wing fillet region at about 30% of the body length. Separation of the flow from the upper surface of the body started just below 10° of incidence and by $\alpha = 15^{\circ}$ was clearly marked (Fig.20), resulting in the formation of body vortices which trailed back down the centre of the model. The separation from the wing leading-edge started a little nearer the nose at the higher incidences but, because the strakes on the side of the body were small and not very sharp, the separation over the range of incidence tested never began ahead of about 25% of the body length. As incidence was increased and the wing vortices grew in strength and moved inboard, they pulled the body vortices down towards the model, so that, following the onset of body asymmetry at $\alpha \simeq 20^{\circ}$, the body vortices wrapped in succession around the port wing vortex (Fig.20). This was clearly demonstrated by the smoke tests.

Similar results were obtained on the model without a fillet. In this configuration, the length of the body overhang was greater and at full-scale the onset of body-vortex asymmetry at zero sideslip might be expected to occur at a lower incidence than that for the layout with fillet. Some of the effects of vortex asymmetry, and the limitations of the small-scale 4 ft × 3 ft tunnel models in assessing the incidence at which asymmetry commences, are discussed in Ref.4.

A noticeable feature of these flow tests made on a sting rig was the steadiness of the wing-body models compared with the ogee models. These latter were so unsteady at the higher incidences that the tunnel speed had to be reduced to 60 ft/sec. Similar problems were experienced with the ogee models in the force tests; and furthermore, some comparative measurements of damping in yaw on a $p = 0.450$ ogee model and a wing-body model have shown that the ogee alone experienced negative damping in yaw at high incidence[4].

3.2 Lift, drag and pitching moments of the basic shapes

The lift, drag and pitching moment coefficients of the four models are given in Tables 3 and 5. These coefficients have been calculated using the areas and aerodynamic mean chords of the whole planform in each case. Lift curves are plotted in Fig.5 for the three ogee wings and in Fig.9 for the complete wing-body model. The lift coefficients for all these models, all having the same slenderness ratio are very similar, though Fig.5 shows a slight tendency for lift at a given incidence to decrease with increasing value of p. At 15° of incidence, the four models have lift coefficients some 6% higher than those from the mean curve drawn in Ref.5 for gothics ($p = 0.667$) and deltas ($p = 0.5$). These latter were flat plate models and Ref.5 shows that taking into account thickness would widen the differences in lift between the present shapes and the pure gothics and deltas. Further systematic work on the effect of planform and thickness on lift is clearly desirable. This is partially being covered by tests at present in progress on a series of wings specially designed to investigate more systematically the effect of planform on aerodynamic centre position.

The lift-dependent drag factor and the lift/drag ratio plotted in Fig.6 for the ogee models (transition free) show little effect on the approach drag within the range of p tested, the difference in lift-dependent drag factor arising mainly from the change in aspect ratio, i.e. K/A is nearly constant. Fig.10 shows some advantage for the wing-body model.

The pitching moments plotted in Fig.7 for the ogees, and in Fig.11 for the wing-body configuration with and without fillets, show the vital importance of careful choice of planform as regards the static longitudinal stability.

3.3 Aerodynamic centre position and attempts to improve the static longitudinal stability

For most of the expected subsonic range of lift coefficient 0.1 to 0.7*, the positions of the aerodynamic centre moves forward with increasing lift coefficient (Fig.13). This forward movement is most marked for the ogee wings, particularly in the C_L range 0.1 to 0.5. In Fig.14 the pitching moment coefficients for the three ogee models and the wing-body model with and without fillets have been replotted about moment centres chosen to give neutral static longitudinal stability at $C_L = 0.5$. It is evident that for the three ogee wings tested the amount of elevator needed to trim at low speed and the amount of camber needed to trim at high speed will be greater than that needed for the wing-body layout, assuming similar rearward movements of aerodynamic centre with Mach number, and no centre of gravity change through the speed range.

Attempts to reduce the rate of forward movement of the aerodynamic centre with lift coefficient were made for both ogee and wing-body layouts. Thus, for the ogee model p = 0.430, six different shapes of extension to the rear of the planform were made, to see if more non-linear lift could be obtained aft of the moment centre by adding to the area beneath the leading-edge vortices (Fig.4(a)). An analysis of the results given in Table 4 and plotted in Fig.8 shows the following changes in static stability margin (Δhn) between $C_L = 0.1$ and 0.7 as compared with the basic wing. Δhn is given as a fraction of the centre-line chord c_o which is the same for all seven configurations.

Basic wing	Wing with extension					
	A	B	C	D	E	F
0.039	0.050	0.044	0.049	0.051	0.038	0.022

Only the large rectangular extension F yields any reduction in the rate of forward movement of the aerodynamic centre.

On the wing-body model the effect of reducing the non-linear lift at the front was tried, the forebody being drooped to reduce the local angle of incidence. Such nose droop is desirable for pilot's view in the approach and

* Assuming an approach lift coefficient in the neighbourhood of 0.5 airworthiness requirements will demand that the aircraft be adequately cleared to $C_L \simeq 0.7$.

to delay the onset of body vortex asymmetry[4]. Results with simple droop angles of 10° and 20°, as well as with a parabolic droop, are plotted in Figs.9 and 12. For these models the changes in the static-stability margin $\Delta hn/c_0$ between $C_L = 0.1$ and 0.7 are listed below.

Basic model	Model cut for droop tests	10° droop	20° droop	Parabolic arc droop
0.015	0.014	0.009	0.008	0.006

The gains due to droop are not large, but are sufficient to ensure that the wing-body layout even with a fillet does have a nearly linear pitching moment v lift relationship.

For both integrated and wing-body layouts the forward movement of the aerodynamic centre with increase of lift will be greater when camber is applied to the wing, but there is some evidence that for cambers producing the same pitching moment increment this change is smaller for the wing-body than the integrated layout[6].

The positions of the aerodynamic centre at a lift coefficient of 0.5 for all the models tested are shown in Fig.15, plotted against the position of the centroid of area of their total planforms. The figure also shows the mean line taken from Ref.7 for thick wings. Analysis of the results with trailing-edge extensions to the p = 0.430 ogee model shows that if the length from the apex of the wing to the centre of the trailing-edge of the extension is used as the reference length in defining the positions of the aerodynamic centre and centroid of area then the aerodynamic centre position of all the variants A-F correlate well with the basic wing position along a line parallel to the line taken from Ref.7.

3.4 Contribution of the body and fillet to the lift and pitching moment of the wing-body model

In Figs.16 and 17 the lift and pitching moment coefficients of the two wing-body models based on the area of the wing alone are plotted together with the results for the wing alone. The effect of the body and fillet on the overall lift of the wing is very small and the lift curve using the new reference area, i.e. that of a mild gothic wing is identical with that taken from Ref.5. A chordwise redistribution of lift is indicated by Figs.16 and 17. This is shown most clearly by the position of the centre of pressure (Fig.18), and although the addition of the body to the wing gave a more constant centre of pressure position through the range of incidence, the subsequent addition of the fillet caused a rapid forward movement of the centre of pressure at the higher incidences. The effect of this latter addition on the aerodynamic centre position is shown in Fig.13.

Since the size of the strakes on the complete model was insufficient to fix the beginning of the leading-edge separation at one point for all incidences, while, with the mid-wing position the wing vortices failed to collect the body vortices at the lower incidences and to prevent them trailing over the fin position, it is considered that fillets of this type serve no useful purpose.

4 CONCLUSIONS

The tests show the effect of a limited range of planform shape variation on the low-speed static longitudinal stability of slender supersonic transports and enable some low-speed aerodynamic comparisons to be made between the integrated and wing-body layouts.

For the three ogee planforms tested, the changes in leading-edge sweep were gradual enough not to impair continuous vortex development along the leading edge. With the wing-body arrangement, flow separations from the body at moderate incidence gave rise to body vortices which trailed back down the centre of the model. At high incidences these body vortices became asymmetric and wrapped round the wing leading-edge vortices. The presence of a planform fillet in the wing-body junction, continued forward as small strakes on the side of the body, yielded no improvements and introduced uncertainty in the position of the start of the wing leading-edge vortices. Further work on other wing-body arrangements not reported here has demonstrated the variations in wing and body vortex interaction which can be obtained as the relative strengths and positions are changed.

All the models tested had the same slenderness ratio and showed virtually no change in lift coefficient, based on the total planform area, within the small range of p tested. These lift coefficients were some 6% higher than those measured earlier for gothic and delta wings of the same slenderness ratio but, assessing the lift coefficient of the wing-body models on the area of the basic wing gave the same lift as measured on the wing alone and on the gothic and delta wings.

Analysis of the pitching moments showed a forward movement of aerodynamic centre with increase of lift on all the models, this being more pronounced for the ogee planforms. Adding wing root planform fillets to the wing-body model increased the forward movement of aerodynamic centre. Attempts to reduce this movement on one of the ogee models by trailing-edge extensions were not very successful. However, on the complete wing-body model drooping the forebody yielded some benefit, and this improvement taken in conjunction with the effect of the fillet indicates that a drooped nose version of the wing-body model without a fillet should be virtually free from forward movement of the aerodynamic centre with incidence.

SYMBOLS

A	aspect ratio = $b^2/S = b/pc_o$
b	span
c_o	centre-line chord of the ogee models and the bodies of the wing-body models
c_{o_w}	centre-line chord of the wing of the wing body model
$\bar{\bar{c}}$	aerodynamic mean chord
C_D	drag coefficient
C_{D_o}	zero-lift drag coefficient
C_L	lift coefficient
C_m	pitching moment coefficient
h_n	longitudinal static stability margin
p	planform parameter = S/bc_o
s	semi-span
s'	local semi-span
S	plan area
V_o	free stream tunnel speed
x	chordwise dimension
y	spanwise dimension
α	incidence (in degrees)

REFERENCES

No.	Author	Title, etc.
1	Earnshaw, P.B.	Low-speed wind-tunnel tests on a series of cambered ogee wings. A.R.C. CP No.775 November 1963
2	Maltby, R.L., Keating, R.F.A.	Flow visualization in low-speed wind-tunnels, current British practice. R.A.E. Tech. Note Aero 2715, ARC 22,373, August 1960.
3	Berndt, S.B.	Wind-tunnel interference due to lift for delta wings of small aspect ratio. K.T.H. Aero Tech. Note 19, 1950.
4	Maltby, R.L., Spence, A.	Some low-speed asymmetry problems on high-speed configurations. Lecture to the Royal Aeronautical Society in February 1962.
5	Peckham, D.H.	Low-speed wind-tunnel tests on a series of uncambered slender pointed wings with sharp edges. A.R.C. R and M 3186, December 1958.
6	Spence, A., Smith, J.H.B.	Some aspects of the low speed and supersonic aerodynamics of lifting slender wings. 3rd ICAS Congress Stockholm, August 1962.
7	Spence, A., Lean, D.	Some low-speed problems of high-speed aircraft. Journal of the Royal Aeronautical Society, Volume 66, No.616, April 1962.

TABLE 1

Details of models

(a) Main dimensions

	Ogee			Wing + body + fillet	Wing + body	Wing
Centre-line chord (c_o) in.	24.67	24.67	24.67	27.75	27.00	19.71
Span (b) in.	10.29	10.29	10.29	11.58	11.27	11.27
Area (S) sq in.	109.2	114.2	118.5	146.2	136.9	127.9
$p = S/bc_o$	0.430	0.450	0.467	0.455	0.450	0.576
$A = b^2/S = b/pc_o$	0.970	0.927	0.894	0.917	0.927	0.993
Aerodynamic mean chord ($\bar{\bar{c}}$) in.	14.85	15.19	15.08	16.18	15.61	13.65
b/c_o	0.417	0.417	0.417	0.417	0.417	0.572
$\bar{\bar{c}}/c_o$	0.602	0.616	0.611	0.583	0.578	0.6925
Distance of moment centre behind apex/c_o	0.6755	0.676	0.6755	0.6595	0.670	0.548
Moment centre for neutral stability at $C_L = 0.5/c_o$ (see Fig.14)	0.680	0.665	0.660	0.6765	0.683	
Distance of centre of area behind apex/c_o	0.699	0.692	0.6945	0.7085	0.711	0.654

TABLE 1 (Continued)

(b) Planform and centre-line thickness of ogee models

Per cent of centre-line chord	Distance from wing apex (in.)	Centre-line i.e. maximum thickness (in.)	Centre radius of transverse section (in.)	$p = 0.430$	Local span $p = 0.450$	(in.) $p = 0.467$
0	0	0	0	0	0	0
5	1.23	0.40	0.20	0.58	0.56	0.60
10	2.47	0.74	0.37	1.00	1.01	1.01
15	3.70	1.01	0.505	1.34	1.39	1.32
20	4.93	1.19	0.595	1.57	1.70	1.57
25	6.17	1.30	0.65	1.82	1.99	1.83
30	7.40	1.33	0.70	2.08	2.27	2.12
35	8.63	1.33	0.74	2.37	2.57	2.47
40	9.87	1.33	0.78	2.66	2.91	2.91
45	11.10	1.33	0.78	2.99	3.32	3.44
50	12.33	1.33	0.78	3.39	3.80	4.05
55	13.57	1.33	0.78	3.92	4.36	4.75
60	14.80	1.33	0.78	4.54	5.01	5.50
65	16.03	1.33	0.78	5.26	5.74	6.30
70	17.27	1.33	0.78	6.08	6.53	7.12
75	18.50	1.25	0.86	7.01	7.36	7.91
80	19.73	1.10	1.04	7.07	8.20	8.66
85	20.97	0.90	1.27	8.88	8.98	9.31
90	22.20	0.68	1.66	9.62	9.64	9.83
95	23.43	0.40	-	10.09	10.11	10.17
100	24.67	0.15	-	10.29	10.29	10.29

All the transverse sections were formed by drawing tangents from the wing edges to the arcs given by the centre radius. The planform of the $p = 0.430$ wing was taken from a project study by Hawker Siddeley Aviation Ltd and the others defined by the relationships

$$s(x) = 1.2\,x - 2.4\,x^2 + 2.2\,x^3 + 3\,x^4 - 3\,x^5$$

for $p = 0.450$

and

$$s(x) = 1.4\,x - 5.3\,x^2 + 12.4\,x^3 - 9.5\,x^4 + 2\,x^5$$

for $p = 0.467$

The leading edge radius was of the order of 0.01 in.

TABLE 1 (Continued)

(c) Planform and centre-line thickness of wing-body models

Per cent of total length	Distance from nose of body (in.)	Local body diameter (in.)	Local span (in.)	Local span without fillet (in.)	Local span of wing (in.)	Centre-line thickness of wing (in.)
0	0	0	0	0	0	0
5.41	1.5	0.49	0.54	0.49		
10.81	3.0	0.89	0.94	0.89		
16.22	4.5	1.215	1.26	1.215		
21.62	6.0	1.44	1.48	1.44		
27.03	7.5	1.63	1.67	1.63	0.005	
32.43	9.0	1.77	1.96	1.77	1.04	0.33
37.84	10.5	1.895	2.49	2.07	2.07	0.565
43.24	12.0	1.975	3.255	3.105	3.105	0.74
48.65	13.5	2.01	4.18	4.135	4.135	0.855
54.05	15.0	1.98	5.16	5.16	5.16	0.925
59.46	16.5	1.92	6.20	6.20	6.20	0.925
64.86	18.0	1.795	7.23	7.23	7.23	0.895
70.27	19.5	1.61	8.23	8.23	8.23	0.835
75.68	21.0	1.385	9.23	9.23	9.23	0.755
81.08	22.5	1.12	10.06	10.06	10.06	0.645
86.49	24.0	0.84	10.78	10.78	10.78	0.505
91.89	25.5	0.515	11.26	11.26	11.26	0.335
100.00	27.75	0	11.575	11.575	11.575	0.02

The above dimensions refer to the 27.75 in. long model. The planform and cross sections for this model were taken from a Bristol Aircraft Ltd design. The dimensions of the 27 in. long model were scaled from the above table. The leading edge radius was of the order of 0.01 in.

TABLE 2

Details of trailing-edge extensions to ogee model, p = 0.430

Extension	Extra length in inches	% of wing span extended	% increase of area	$\bar{\bar{c}}$ with extensions / $\bar{\bar{c}}_{basic}$
A	0.91	100	4.29	0.999
B	1.87	100	8.80	1.000
C	0.92	$66\frac{2}{3}$	2.88	0.991
D	1.98	$66\frac{2}{3}$	6.22	0.983
E	0.92	$66\frac{2}{3}$	5.77	0.997
F	1.98	$66\frac{2}{3}$	12.44	1.000

TABLE 3

Lift, drag and pitching moment coefficients of the ogee models

α^o	C_L	C_D	C_m	$\frac{C_D - C_{D_o}}{C_L^2 / \pi A}$	L/D
p = 0.430 (moment centre at 0.6755 c_o)					
V_o = 200.2 ft/sec					
-3.95	-0.096	0.0142	0.0060	2.18	-6.76
-1.95	-0.046	0.0094	0.0026	2.59	-4.89
+0.2	+0.004	0.0076	-0.0002	-	+0.53
2.25	0.051	0.0101	-0.0027	2.93	5.05
4.3	0.110	0.0158	-0.0065	2.06	6.96
6.25	0.171	0.0254	-0.0101	1.86	6.73
8.35	0.240	0.0406	-0.0135	1.75	5.91
10.3	0.312	0.0606	-0.0165	1.66	5.15
12.45	0.394	0.0897	-0.0186	1.61	4.39
14.35	0.474	0.1232	-0.0202	1.57	3.85
16.5	0.559	0.1660	-0.0209	1.54	3.37
18.45	0.641	0.2135	-0.0203	1.53	3.00
20.55	0.725	0.2709	-0.0191	1.53	2.68
V_o = 100.5 ft/sec					
18.6	0.647	0.2162	-0.0213	1.52	2.99
20.6	0.750	0.2712	-0.0202	1.51	2.69
22.65	0.814	0.334	-0.0198	1.50	2.44
24.6	0.891	0.3985	-0.0190	1.50	2.24
26.65	0.972	0.4795	-0.0188	1.52	2.03
p = 0.450 (moment centre at 0.676 c_o)					
V_o = 200.2 ft/sec					
-3.75	-0.090	0.0141	0.0030	2.19	-6.57
-1.7	-0.038	0.0097	0.0010	3.54	-4.09
+0.25	+0.004	0.0080	0.0002	-	+0.53
2.25	0.051	0.0102	-0.0015	2.46	5.20
4.3	0.107	0.0161	-0.0034	2.06	6.82
6.35	0.169	0.0256	-0.0045	1.79	6.71
8.4	0.238	0.0407	-0.0059	1.68	5.91
10.45	0.313	0.0619	-0.0063	1.60	5.09
12.45	0.393	0.0901	-0.0061	1.55	4.38
14.55	0.477	0.1258	-0.0049	1.51	3.80
16.65	0.559	0.1667	-0.0033	1.48	3.36
18.6	0.643	0.2151	-0.0008	1.46	2.99
20.65	0.726	0.2714	+0.0031	1.46	2.68

TABLE 3 (Continued)

α^o	C_L	C_D	C_m	$\dfrac{C_D - C_{D_o}}{C_L^2/\pi A}$	L/D
V_o = 100.5 ft/sec					
10.5	0.316	0.0629	-0.0062	1.60	5.06
14.6	0.481	0.1298	-0.0042	1.53	3.72
18.7	0.650	0.2188	-0.0003	1.45	2.98
20.65	0.735	0.2737	+0.0008	1.43	2.69
22.75	0.824	0.3385	0.0067	1.42	2.44
24.75	0.901	0.4055	0.0077	1.43	2.22
26.85	0.985	0.4865	0.0125	1.44	2.03
p = 0.467 (moment centre at 0.6755 c_o)					
V_o = 200.2 ft/sec					
-4.05	-0.096	0.0136	0.0011	1.83	-7.06
-2.0	-0.044	0.0092	0.0001	2.32	-4.78
0	0	0.0076	0	-	0
+2.0	+0.043	0.0098	-0.0001	3.34	+4.39
4.05	0.098	0.0150	-0.0010	2.16	6.53
6.0	0.156	0.0232	-0.0015	1.80	6.72
8.15	0.225	0.0374	-0.0018	1.65	6.02
10.15	0.297	0.0568	-0.0019	1.57	5.23
12.25	0.377	0.0836	-0.0004	1.50	4.51
14.3	0.460	0.1173	+0.0015	1.46	3.92
16.3	0.540	0.1553	0.0034	1.42	3.48
18.4	0.636	0.2082	0.0062	1.39	3.05
20.35	0.719	0.2617	0.0103	1.38	2.75
V_o = 100.5 ft/sec					
10.25	0.302	0.0590	-0.0029	1.58	5.12
14.35	0.464	0.1196	+0.0021	1.46	3.88
18.45	0.642	0.2130	0.0072	1.40	3.01
20.5	0.734	0.2696	0.0097	1.37	2.72
22.5	0.822	0.334	0.0158	1.36	2.46
24.55	0.914	0.4085	0.0191	1.35	2.24
26.7	0.998	0.487	0.0240	1.35	2.05

* Note C_D was reduced by 0.0004 in determining L/D for the p = 0.450 ogee because the C_{D_o} for this wing was 0.0080 compared with 0.0076 for the two others.

TABLE 4

Lift, drag and pitching moment coefficients of the ogee model p = 0.430 with trailing-edge extensions

(Moment centre at 0.6755 c_o. Total areas used to non-dimensionalize results, see Table 2)

α^o	C_L	C_D	C_m
Extension A			
V_o = 200.2 ft/sec			
-3.85	-0.090	0.0119	+0.0062
-1.8	-0.038	0.0090	+0.0027
+0.2	+0.005	0.0084	-0.0002
2.3	0.052	0.0114	-0.0037
4.3	0.109	0.0172	-0.0090
6.35	0.179	0.0286	-0.0150
8.4	0.249	0.0447	-0.0199
10.45	0.328	0.0682	-0.0249
12.5	0.406	0.0972	-0.0285
14.55	0.488	0.1329	-0.0313
16.6	0.568	0.1743	-0.0332
18.6	0.655	0.2274	-0.0343
20.7	0.742	0.2875	-0.0347
V_o = 100.5 ft/sec			
18.65	0.660	0.2296	-0.0341
20.65	0.730	0.2795	-0.0348
22.75	0.814	0.3445	-0.0365
24.85	0.901	0.419	-0.0393
26.85	0.986	0.501	-0.0402
Extension B			
V_o = 200.2 ft/sec			
-3.8	-0.090	0.0126	+0.0083
-1.75	-0.038	0.0089	+0.0029
+0.25	+0.005	0.0080	-0.0004
2.3	0.052	0.0105	-0.0042
4.25	0.108	0.0159	-0.0100
6.35	0.179	0.0267	-0.0171
8.45	0.250	0.0427	-0.0236
10.45	0.330	0.0649	-0.0299
12.5	0.402	0.0922	-0.0347
14.55	0.486	0.1279	-0.0398
16.6	0.572	0.1714	-0.0440
18.6	0.655	0.2210	-0.0469
20.7	0.741	0.2794	-0.0497

TABLE 4 (Continued)

α^o	C_L	C_D	C_m
V_o = 100.5 ft/sec			
18.65	0.663	0.2249	-0.0488
20.75	0.748	0.2829	-0.0503
22.75	0.834	0.349	-0.0539
24.8	0.926	0.4205	-0.0596
26.9	1.003	0.504	-0.0633
Extension C			
V_o = 200.2 ft/sec			
-3.8	-0.090	0.0127	+0.0054
-1.75	-0.039	0.0097	+0.0025
+0.20	+0.005	0.0088	-0.0006
2.3	0.054	0.0118	-0.0040
4.25	0.112	0.0176	-0.0092
6.4	0.181	0.0288	-0.0147
8.35	0.248	0.0446	-0.0189
10.45	0.324	0.0673	-0.0228
12.5	0.403	0.0959	-0.0256
14.5	0.483	0.1312	-0.0278
16.6	0.566	0.1743	-0.0292
18.65	0.654	0.2282	-0.0292
20.8	0.734	0.2833	-0.0292
V_o = 100.5 ft/sec			
18.6	0.652	0.2254	-0.0302
20.75	0.734	0.2833	-0.0299
22.75	0.816	0.345	-0.0307
24.8	0.898	0.417	-0.0313
26.8	0.976	0.4925	-0.0323
Extension D			
V_o = 200.2 ft/sec			
-3.85	-0.095	0.0129	+0.0085
-1.75	-0.041	0.0097	+0.0031
+0.3	+0.006	0.0086	-0.0006
2.3	0.052	0.0117	-0.0044
4.25	0.112	0.0185	-0.0103
6.35	0.181	0.0286	-0.0170
8.4	0.252	0.0446	-0.0229
10.45	0.332	0.0685	-0.0286
12.5	0.410	0.0974	-0.0323
14.5	0.492	0.1336	-0.0357
16.6	0.580	0.1795	-0.0382
18.7	0.664	0.2307	-0.0391
20.7	0.742	0.2843	-0.0401

TABLE 4 (Continued)

α°	C_L	C_D	C_m
V_o = 100.5 ft/sec			
18.65	0.671	0.2321	-0.0408
20.7	0.748	0.2863	-0.0397
22.7	0.833	0.3505	-0.0433
24.75	0.925	0.423	-0.0466
26.8	0.997	0.5005	-0.0489
Extension E			
V_o = 200.2 ft/sec			
-3.75	-0.088	0.0126	+0.0077
-1.75	-0.037	0.0094	+0.0032
+0.3	+0.006	0.0083	-0.0004
2.3	0.053	0.0113	-0.0039
4.25	0.112	0.0170	-0.0094
6.3	0.175	0.0269	-0.0149
8.4	0.248	0.0434	-0.0202
10.45	0.322	0.0653	-0.0253
12.5	0.402	0.0939	-0.0300
14.55	0.488	0.1310	-0.0343
16.65	0.574	0.1756	-0.0379
18.6	0.658	0.2210	-0.0393
20.7	0.741	0.2803	-0.0419
V_o = 100.5 ft/sec			
18.6	0.660	0.2261	-0.0407
20.75	0.757	0.2851	-0.0434
22.75	0.832	0.350	-0.0446
24.85	0.916	0.4225	-0.0473
26.85	0.998	0.5005	-0.0513
Extension F			
V_o = 200.2 ft/sec			
-3.8	-0.088	0.0158	+0.0109
-1.75	-0.036	0.0100	+0.0041
+0.25	+0.007	0.0087	-0.0004
2.2	0.049	0.0100	-0.0044
4.25	0.104	0.0141	-0.0098
6.3	0.170	0.0232	-0.0163
8.4	0.241	0.0379	-0.0227
10.45	0.323	0.0605	-0.0306
12.5	0.398	0.0863	-0.0364

TABLE 4 (Continued)

α°	C_L	C_D	C_m
14.55	0.476	0.1181	-0.0426
16.6	0.568	0.1628	-0.0494
18.7	0.662	0.2162	-0.0555
20.7	0.748	0.2733	-0.0605
V_o = 100.5 ft/sec			
18.65	0.659	0.2130	-0.0583
20.65	0.742	0.2674	-0.0626
22.8	0.834	0.334	-0.0693
24.85	0.916	0.4035	-0.0740

TABLE 5

Lift, drag and pitching moment coefficient of the wing-body model with and without fillets

α°	C_L	C_D	C_m	$\dfrac{C_D - C_{D_o}}{C_L^2 / \pi A}$	L/D
(a) With fillet, p = 0.455. Moment centre at 0.6595 c_o					
V_o = 200.4 ft/sec					
-3.95	-0.095	0.0134	0.0045	2.08	-7.09
-1.95	-0.044	0.0089	0.0019	2.98	-4.94
+0.1	+0.003	0.0069	-0.0002	-	+0.43
2.15	0.049	0.0092	-0.0018	2.76	5.33
4.2	0.108	0.0132	-0.0042	2.00	7.20
6.25	0.171	0.0249	-0.0073	1.77	6.87
8.3	0.243	0.0403	-0.0105	1.63	6.03
10.35	0.317	0.0611	-0.0130	1.55	5.19
12.4	0.396	0.0884	-0.0159	1.50	4.48
14.45	0.480	0.1230	-0.0192	1.45	3.90
16.55	0.568	0.1658	-0.0213	1.42	3.43
18.6	0.656	0.2162	-0.0240	1.40	3.03
20.65	0.743	0.2724	-0.0258	1.38	2.73
22.7	0.835	0.3395	-0.0273	1.37	2.46
24.8	0.923	0.416	-0.0270	1.38	2.22

TABLE 5 (Continued)

α^{o}	C_L	C_D	C_m	$\dfrac{C_D - C_{D_o}}{C_L^2/\pi A}$	L/D
(b) Without fillet, p = 0.450. Moment centre at 0.670 c_o					
V_o = 200.5 ft/sec					
-3.45	-0.080	0.0113	0.0021	3.09	-5.93
-1.3	-0.032	0.0082	0.0008	4.27	-3.90
-0.25	-0.006	0.0065	0.0001		-0.92
+0.65	+0.016	0.0071	-0.0006	4.55	+2.250
1.7	0.038	0.0080	-0.0008	2.62	4.75
2.8	0.066	0.0095	-0.0016	1.87	6.95
3.75	0.094	0.0119	-0.0026	1.71	7.90
4.8	0.128	0.0162	-0.0032	1.69	7.90
5.8	0.161	0.0217	-0.0039	1.68	7.42
6.85	0.192	0.0272	-0.0054	1.62	7.06
8.9	0.264	0.0438	-0.0082	1.55	6.03
10.95	0.341	0.0666	-0.0101	1.50	5.12
13.05	0.424	0.0975	-0.0126	1.48	4.35
15.1	0.510	0.1338	-0.0149	1.42	3.81
17.15	0.599	0.1801	-0.0164	1.41	3.33
19.25	0.690	0.2326	-0.0182	1.38	2.97
21.25	0.779	0.2929	-0.0201	1.37	2.66
22.55	0.834	0.333	-0.0210	1.36	2.50
24.65	0.930	0.411	-0.0215	1.36	2.26

TABLE 6

Effect of nose droop on the lift, drag and pitching moment coefficients of the wing-body model

(with fillet, moment centre at 0.6595 c_o)

α^o	C_L	C_D	C_m
No droop			
V_o = 200.4 ft/sec			
-2.35	-0.067	0.0111	0.0028
-1.75	-0.039	0.0096	0.0011
-0.75	-0.017	0.0081	0.0007
+0.3	+0.006	0.0076	-0.0002
1.25	0.026	0.0088	-0.0007
2.3	0.052	0.0097	-0.0019
4.4	0.112	0.0157	-0.0049
6.4	0.174	0.0252	-0.0076
8.45	0.241	0.0400	-0.0104
10.5	0.315	0.0585	-0.0133
12.6	0.395	0.0883	-0.0165
14.65	0.482	0.1243	-0.0200
16.65	0.568	0.1669	-0.0223
18.8	0.660	0.2175	-0.0245
20.8	0.746	0.2740	-0.0267
22.85	0.833	0.3405	-0.0268
24.95	0.916	0.412	-0.0266
27.0	0.999	0.492	-0.0273
10^o droop			
V_o = 200.4 ft/sec			
-2.75	-0.065	0.0125	0
-1.85	-0.042	0.0105	-0.0009
-0.75	-0.018	0.0090	-0.0016
+0.25	+0.004	0.0084	-0.0026
1.25	0.027	0.0095	-0.0033
2.35	0.054	0.0107	-0.0047
4.35	0.108	0.0158	-0.0067
6.45	0.172	0.0257	-0.0098
8.45	0.241	0.0400	-0.0133
10.5	0.316	0.0611	-0.0164
12.55	0.390	0.0865	-0.0197
14.6	0.478	0.1227	-0.0238
16.65	0.561	0.1656	-0.0269
18.75	0.653	0.2062	-0.0306
20.85	0.741	0.2655	-0.0337
22.85	0.830	0.329	-0.0362
24.95	0.920	0.393	-0.0395
27.0	1.004	0.459	-0.0418

TABLE 6 (Continued)

α^o	C_L	C_D	C_m
20^o droop			
V_o = 200.4 ft/sec			
-2.8	-0.065	0.0153	-0.0061
-1.8	-0.043	0.0133	-0.0065
-0.75	-0.020	0.0117	-0.0061
+0.25	+0.001	0.0107	-0.0062
1.2	0.023	0.0112	-0.0063
2.3	0.051	0.0120	-0.0069
4.3	0.105	0.0161	-0.0091
6.45	0.171	0.0261	-0.0122
8.5	0.240	0.0410	-0.0159
10.45	0.308	0.0592	-0.0185
12.5	0.387	0.0859	-0.0220
14.6	0.467	0.1182	-0.0260
16.65	0.559	0.1623	-0.0295
18.75	0.646	0.2102	-0.0327
20.8	0.736	0.2674	-0.0363
22.85	0.826	0.333	-0.0393
24.95	0.914	0.404	-0.0420
26.5	0.979	0.467	-0.0449
Shaped droop			
V_o = 200.4 ft/sec			
-2.65	-0.062	0.0122	0.0004
-1.65	-0.035	0.0103	-0.0006
-0.6	-0.014	0.0093	-0.0009
+0.4	+0.009	0.0087	-0.0019
1.4	0.031	0.0098	-0.0023
2.45	0.057	0.0111	-0.0032
4.5	0.114	0.0169	-0.0057
6.55	0.178	0.0270	-0.0085
8.55	0.247	0.0419	-0.0115
10.65	0.321	0.0626	-0.0145
12.7	0.404	0.0916	-0.0179
14.75	0.488	0.1268	-0.0208
16.9	0.574	0.1695	-0.0242
18.9	0.662	0.2198	-0.0276
21.0	0.755	0.2787	-0.0309
23.0	0.840	0.342	-0.0338
25.1	0.928	0.4165	-0.0357
27.15	1.015	0.498	-0.0384

TABLE 7

Lift, drag and pitching moment coefficients of the wing alone

(Moment centre at 0.548 c_{o_w} corresponding to 0.670 c_o of the wing + body models)

α^o	C_L	C_D	C_m	$\frac{C_D - C_{D_o}}{C_L^2/\pi A}$	L/D
V_o = 200.5 ft/sec					
-3.35	-0.084	0.0106	0.0017	2.034	-7.92
-2.0	-0.048	0.0079	0.0009	2.571	-6.08
-1.0	-0.024	0.0067	0.0005	3.791	-3.58
+0.05	0	0.0054	0	-	-
1.0	+0.028	0.0068	-0.0008	3.183	4.12
2.05	0.053	0.0080	-0.0014	2.221	6.62
3.0	0.080	0.0096	-0.0024	1.755	8.33
4.0	0.112	0.0128	-0.0037	1.691	8.75
5.1	0.149	0.0177	-0.0053	1.644	8.42
6.05	0.183	0.0231	-0.0064	1.593	7.92
8.1	0.259	0.0397	-0.0097	1.567	6.52
10.2	0.341	0.0624	-0.0120	1.513	5.46
12.3	0.429	0.0926	-0.0140	1.468	4.63
14.35	0.519	0.1305	-0.0159	1.442	3.98
16.35	0.606	0.1728	-0.0178	1.417	3.51
18.45	0.715	0.2334	-0.0192	1.388	3.06
20.45	0.804	0.2911	-0.0191	1.376	2.76
22.65	0.908	0.3675	-0.0190	1.368	2.47
24.7	1.005	0.446	-0.0188	1.358	2.25

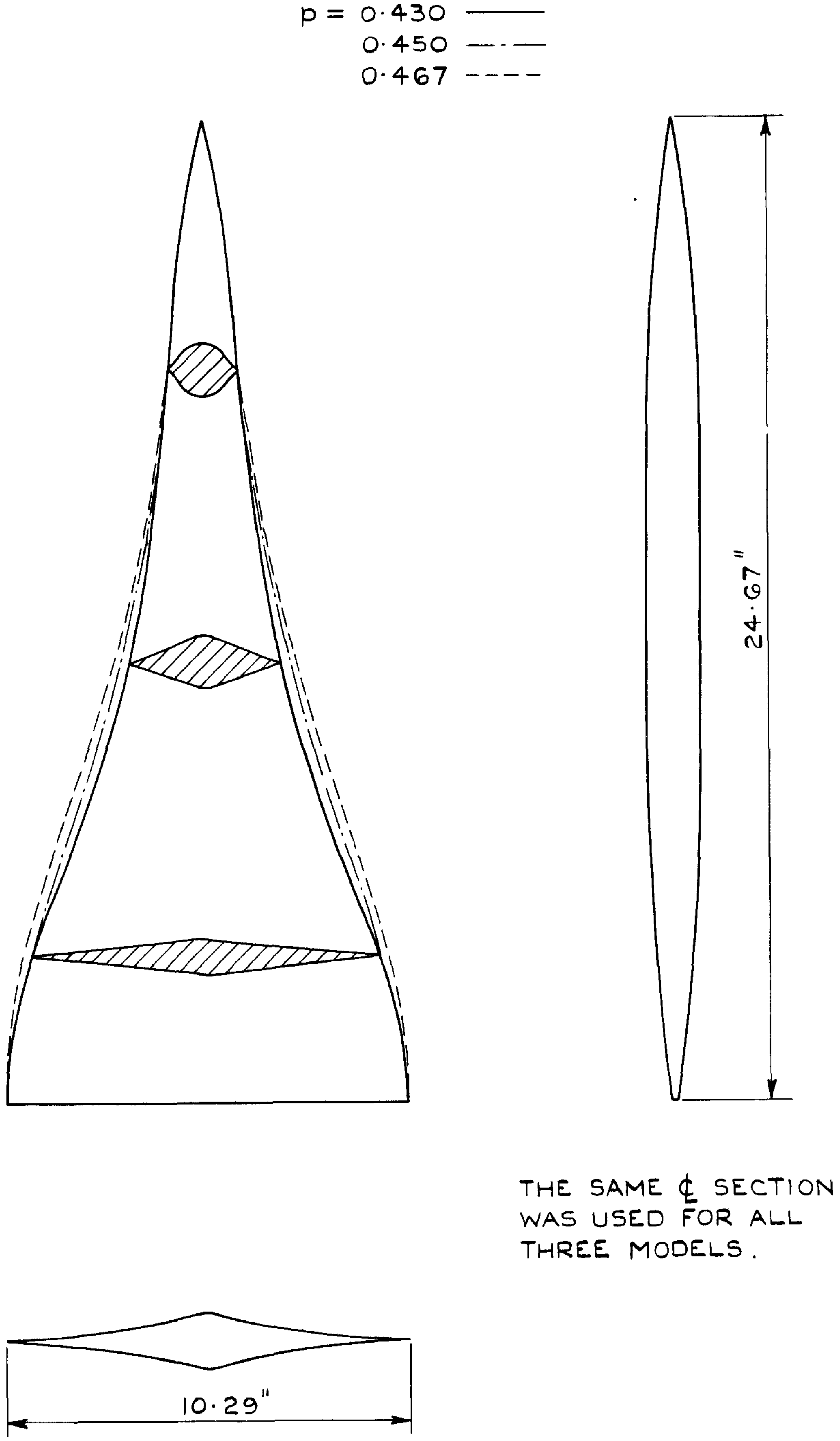

FIG. 1. OGEE MODELS.

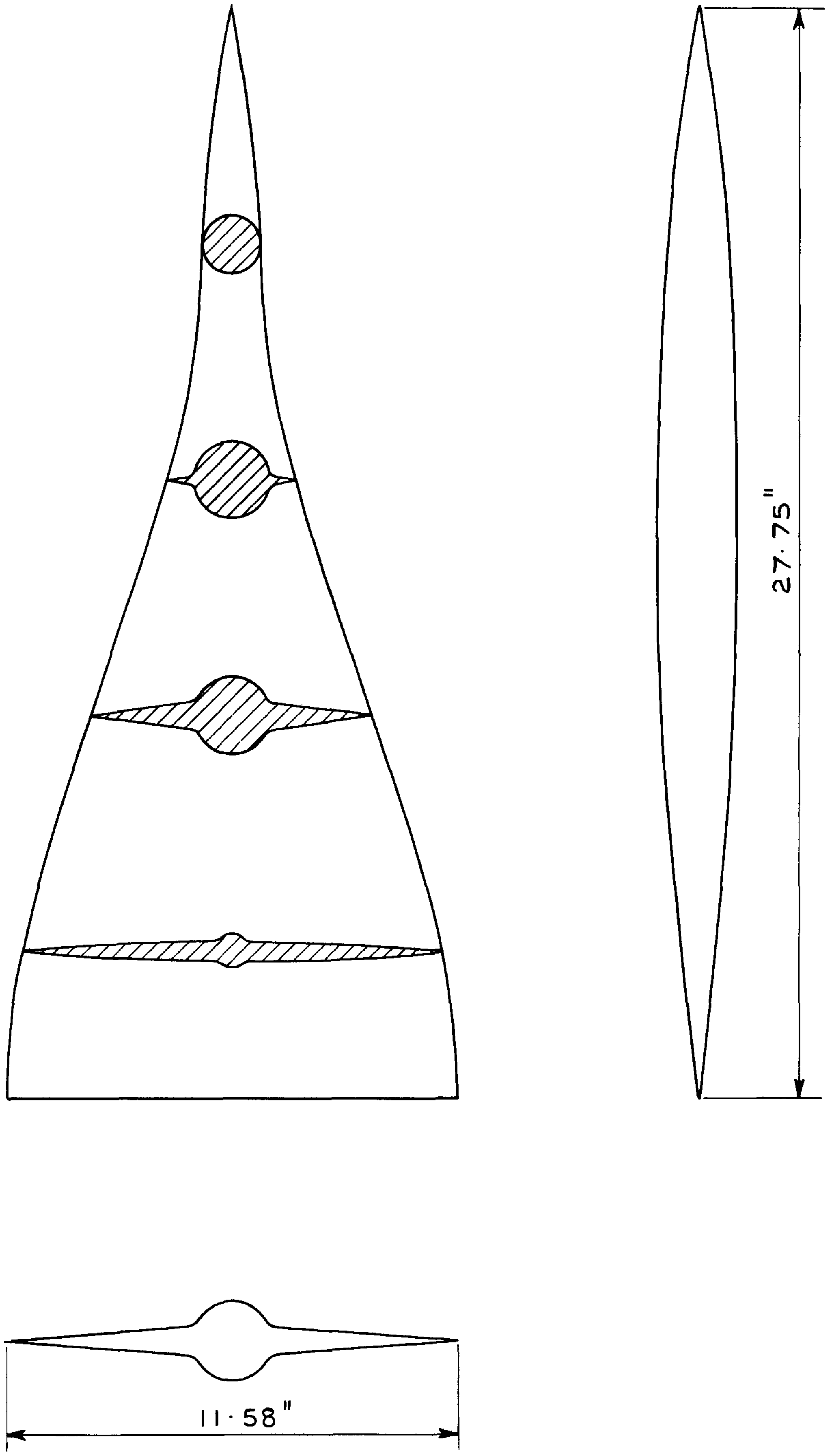

FIG. 2. WING-BODY MODEL.
WITH FILLET.

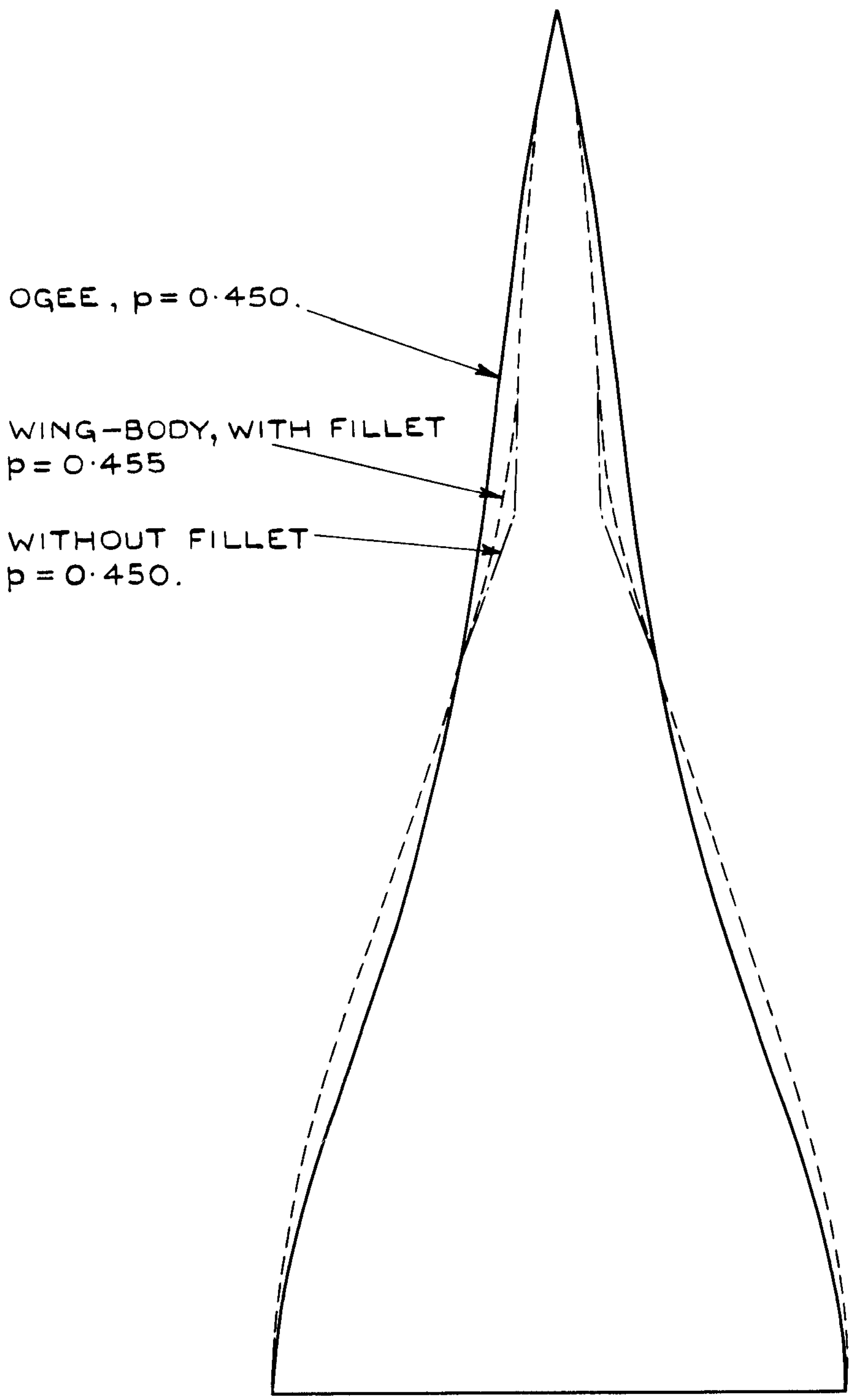

FIG. 3 PLANFORM COMPARISON OF $p = 0{\cdot}450$ OGEE MODEL AND THE WING-BODY MODEL WITH AND WITHOUT FILLET.

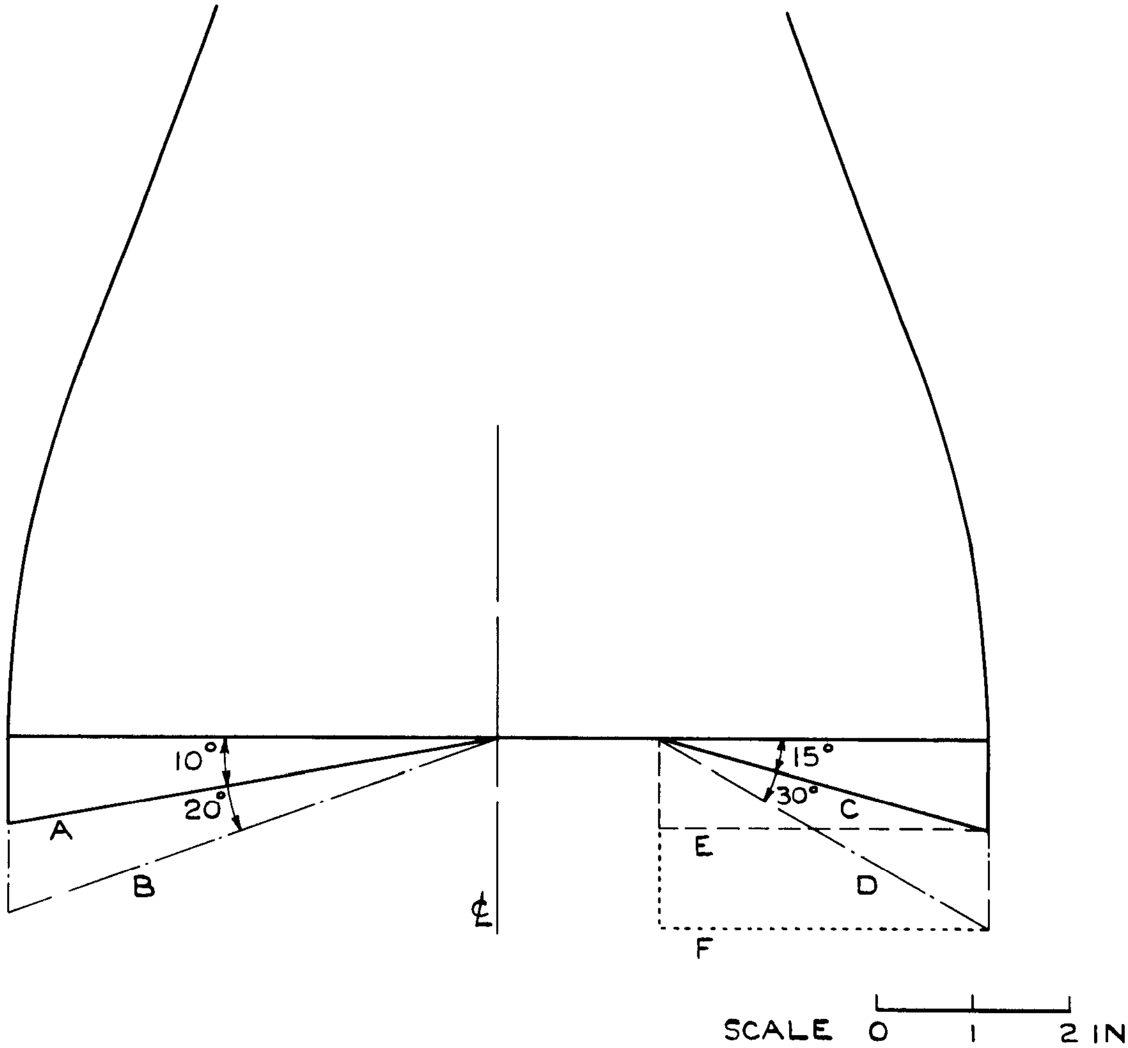

FIG. 4.(a) TRAILING-EDGE EXTENSIONS TO OGEE MODEL, $p = 0{\cdot}430$.

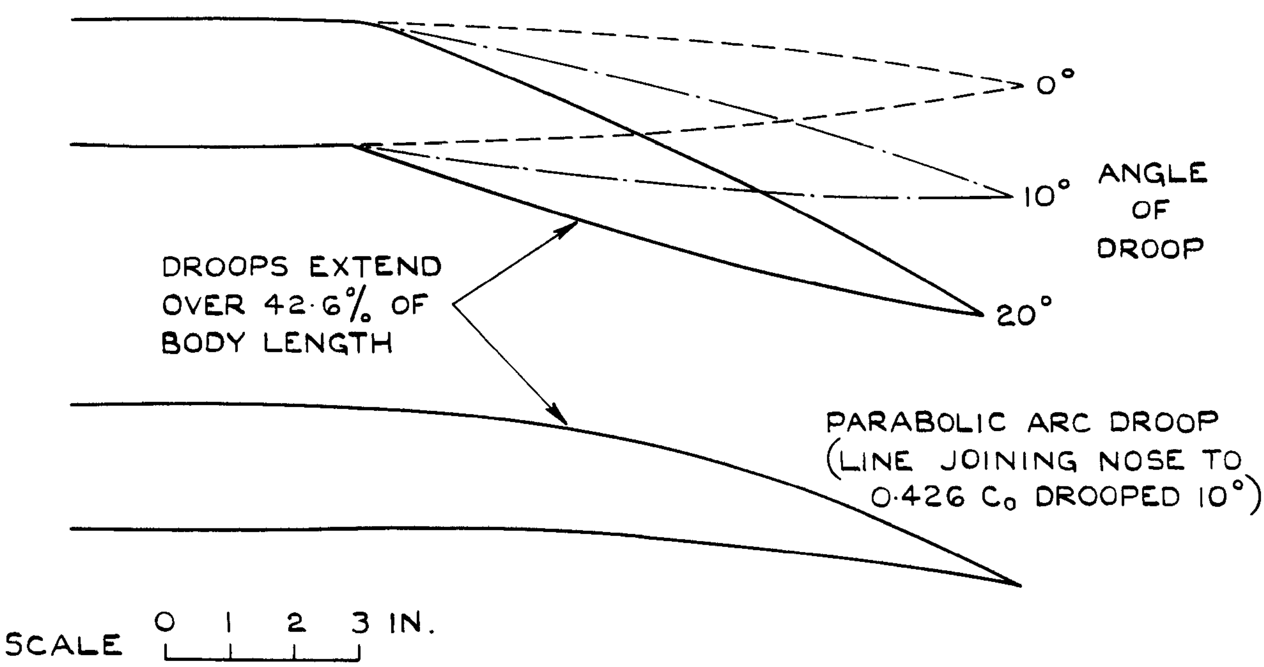

FIG. 4.(b) NOSE DROOP ON WING - BODY MODEL WITH FILLET.

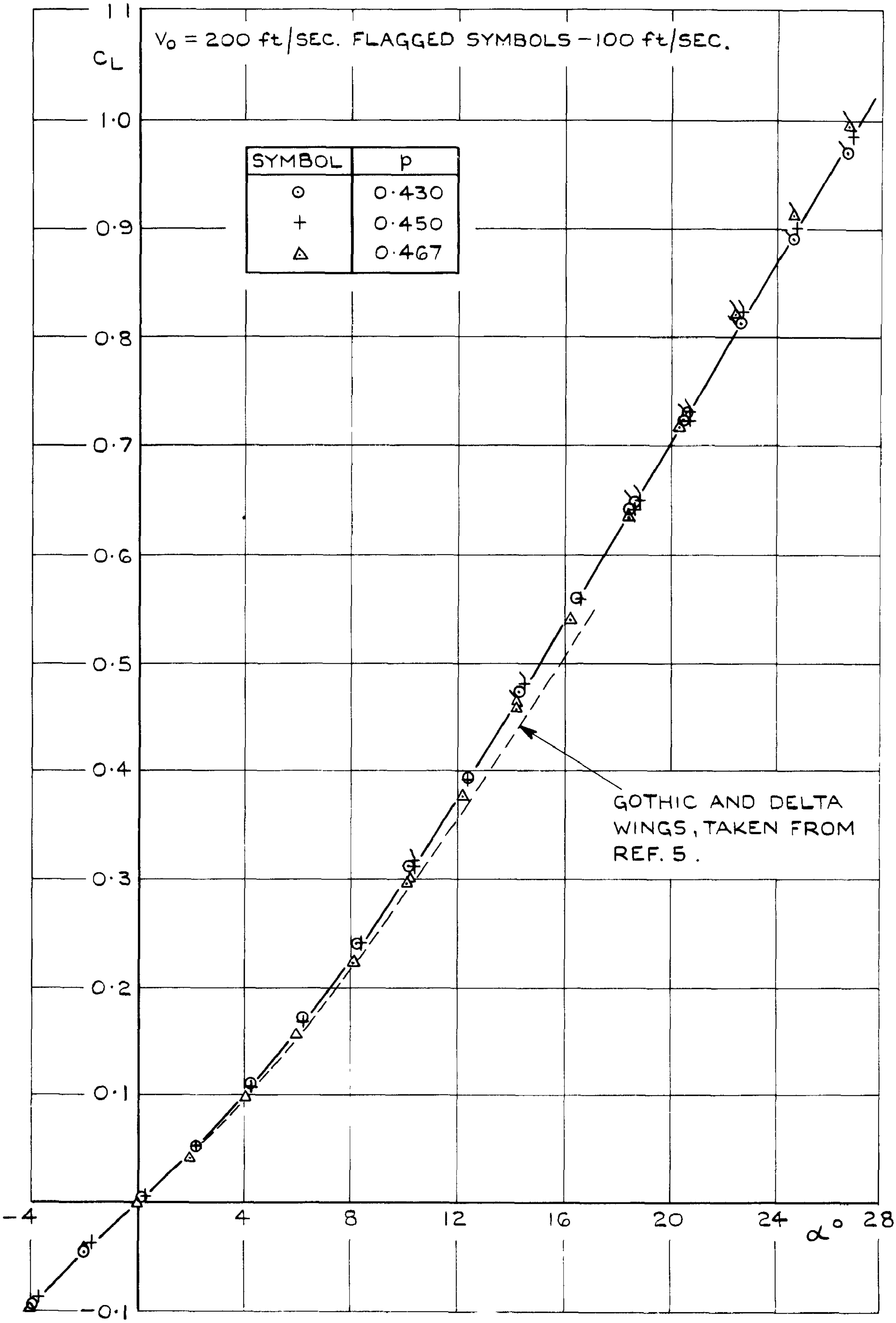

FIG. 5. LIFT COEFFICIENTS OF THE OGEE MODELS.

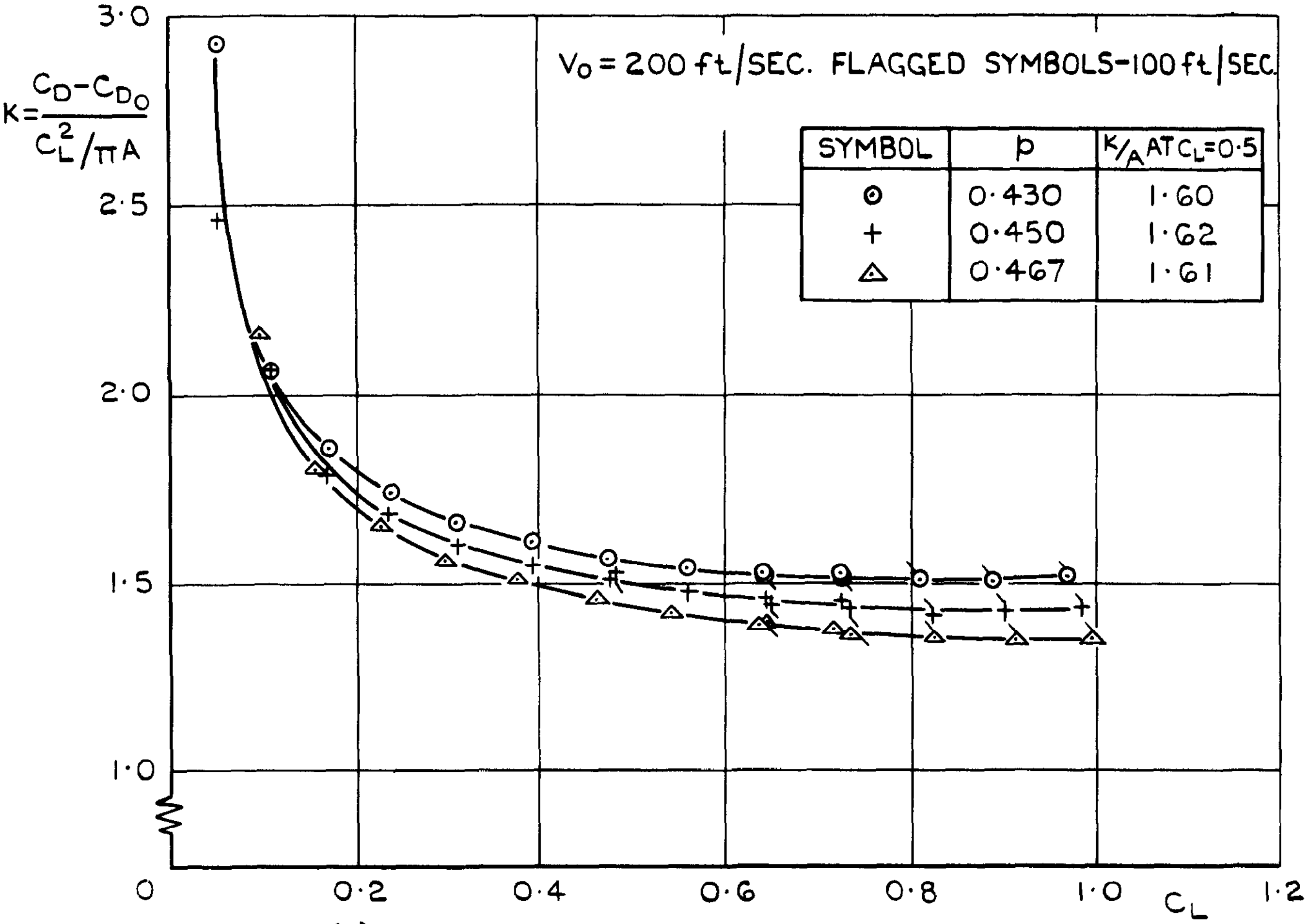

(a) LIFT DEPENDENT DRAG FACTOR.

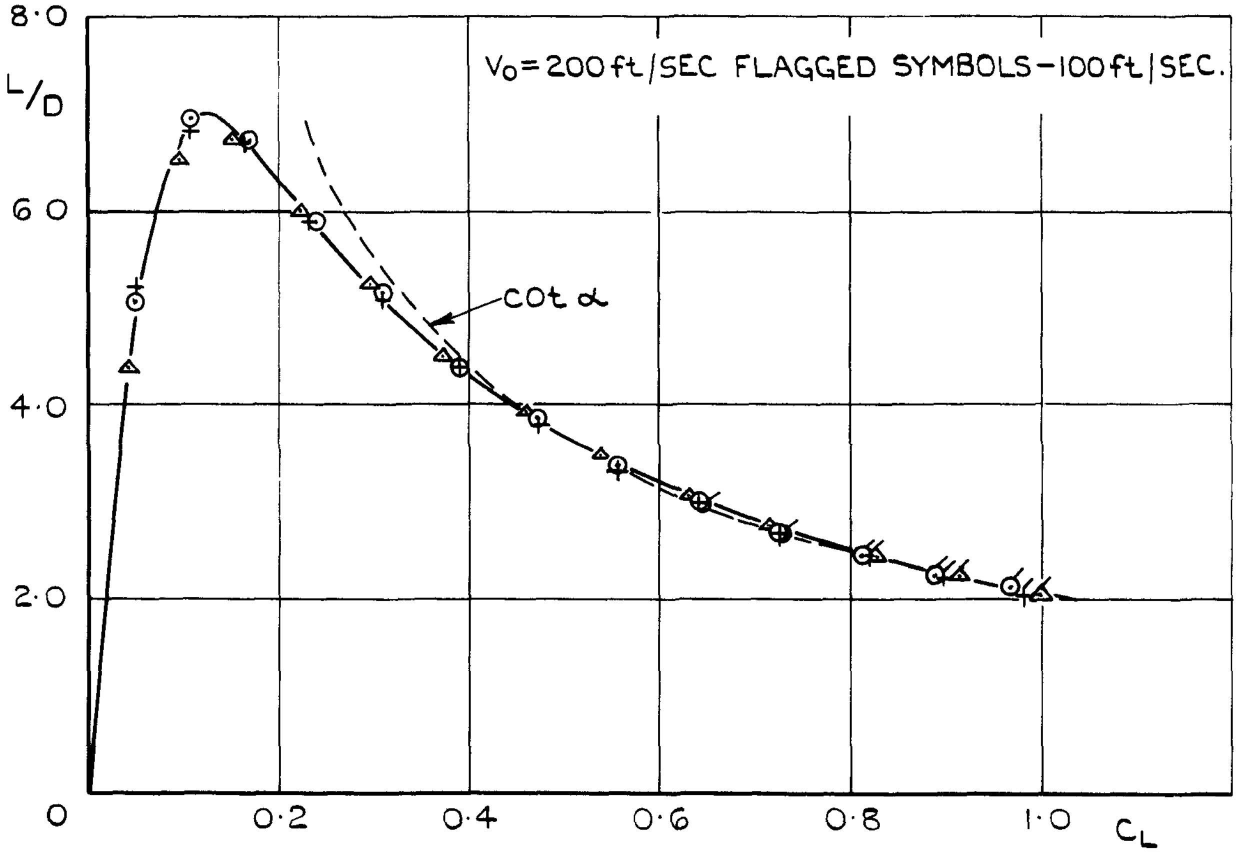

(b) LIFT/DRAG RATIO.

FIG. 6. DRAG CHARACTERISTICS OF THE OGEE MODELS.

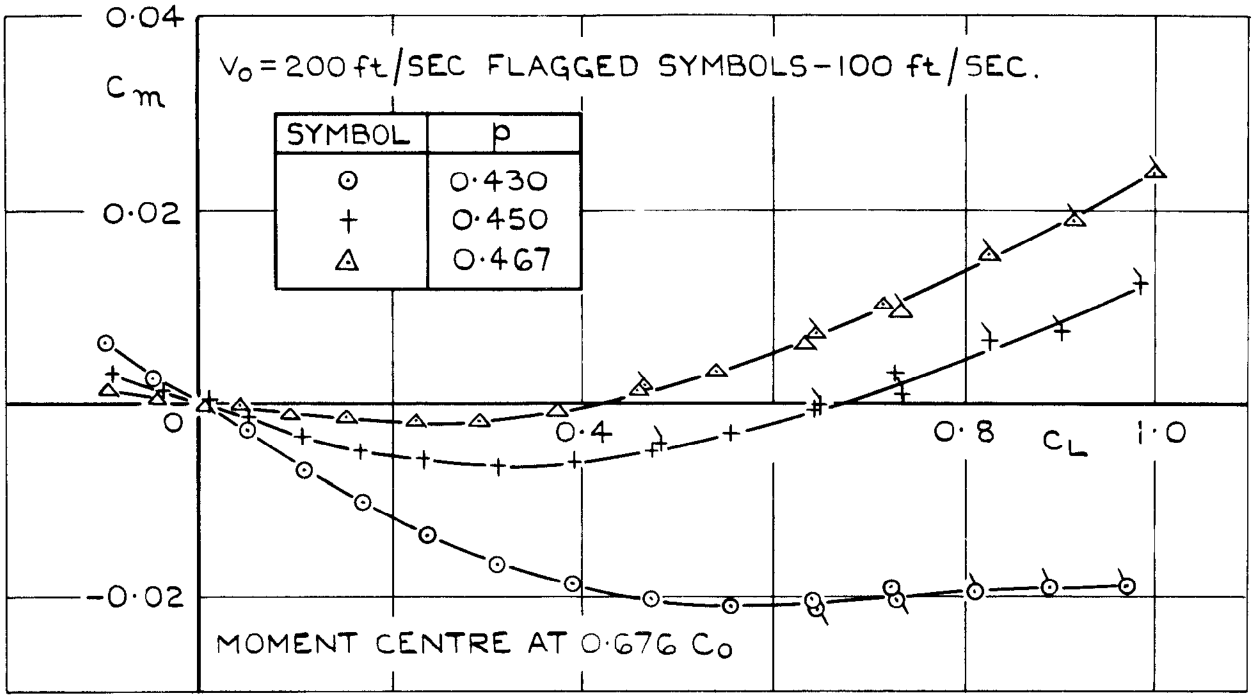

FIG. 7. PITCHING MOMENT COEFFICIENTS, OGEE MODELS

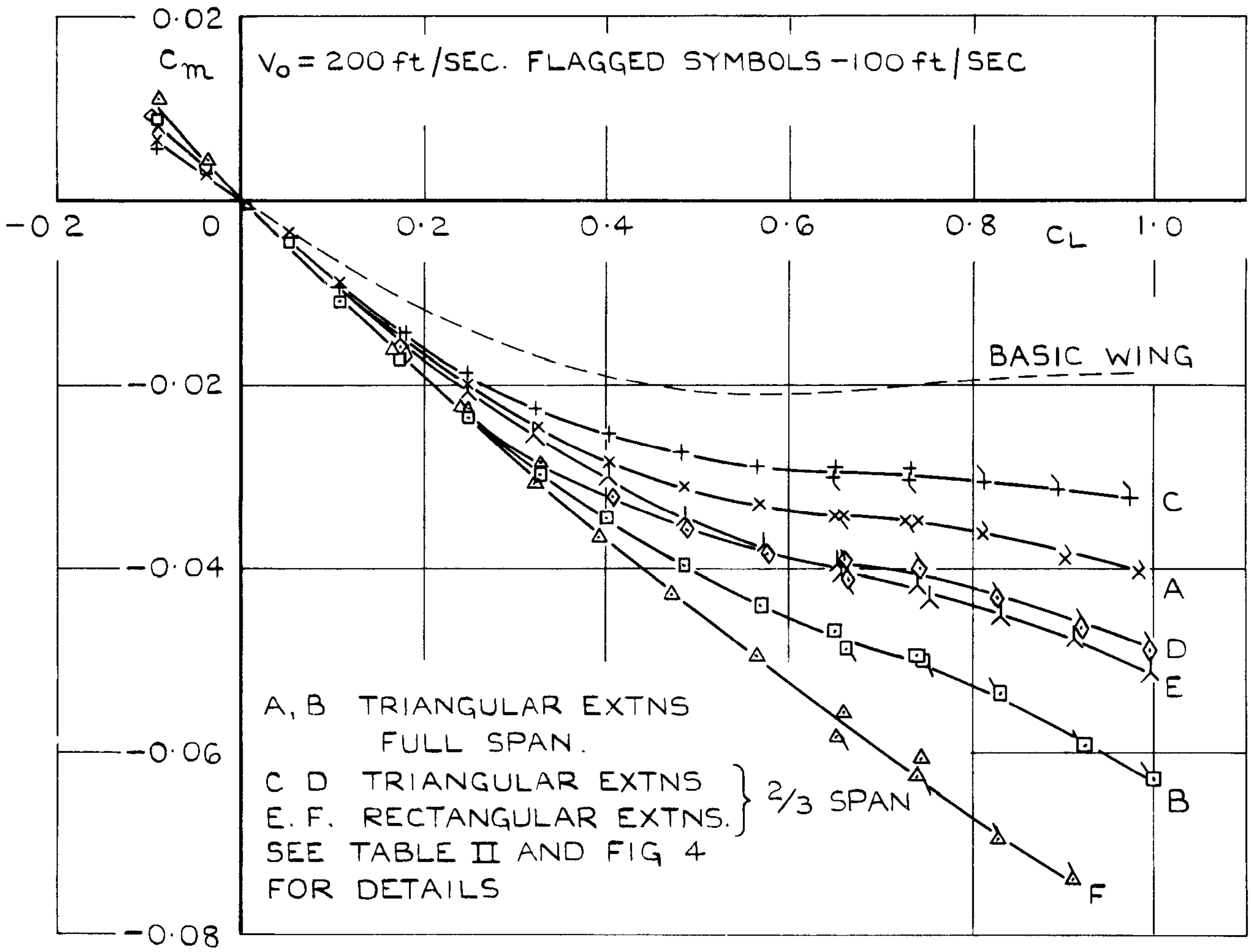

FIG. 8. EFFECT OF PLANFORM CHANGES ON THE PITCHING MOMENTS OF THE $p = 0{\cdot}430$ OGEE MODEL.

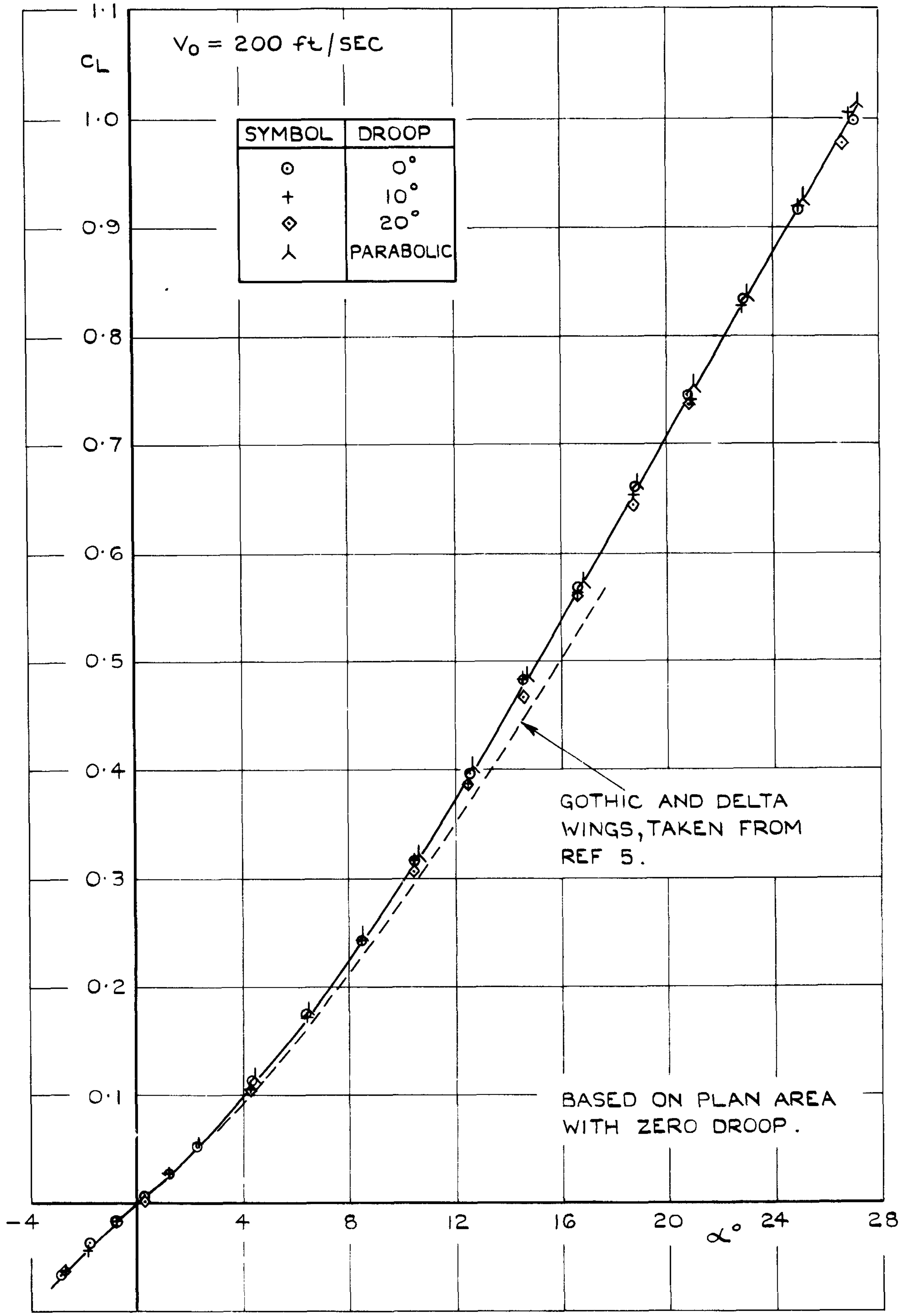

FIG. 9. LIFT COEFFICIENTS OF THE WING-BODY MODEL WITH NOSE DROOP
MODEL WITH FILLET.

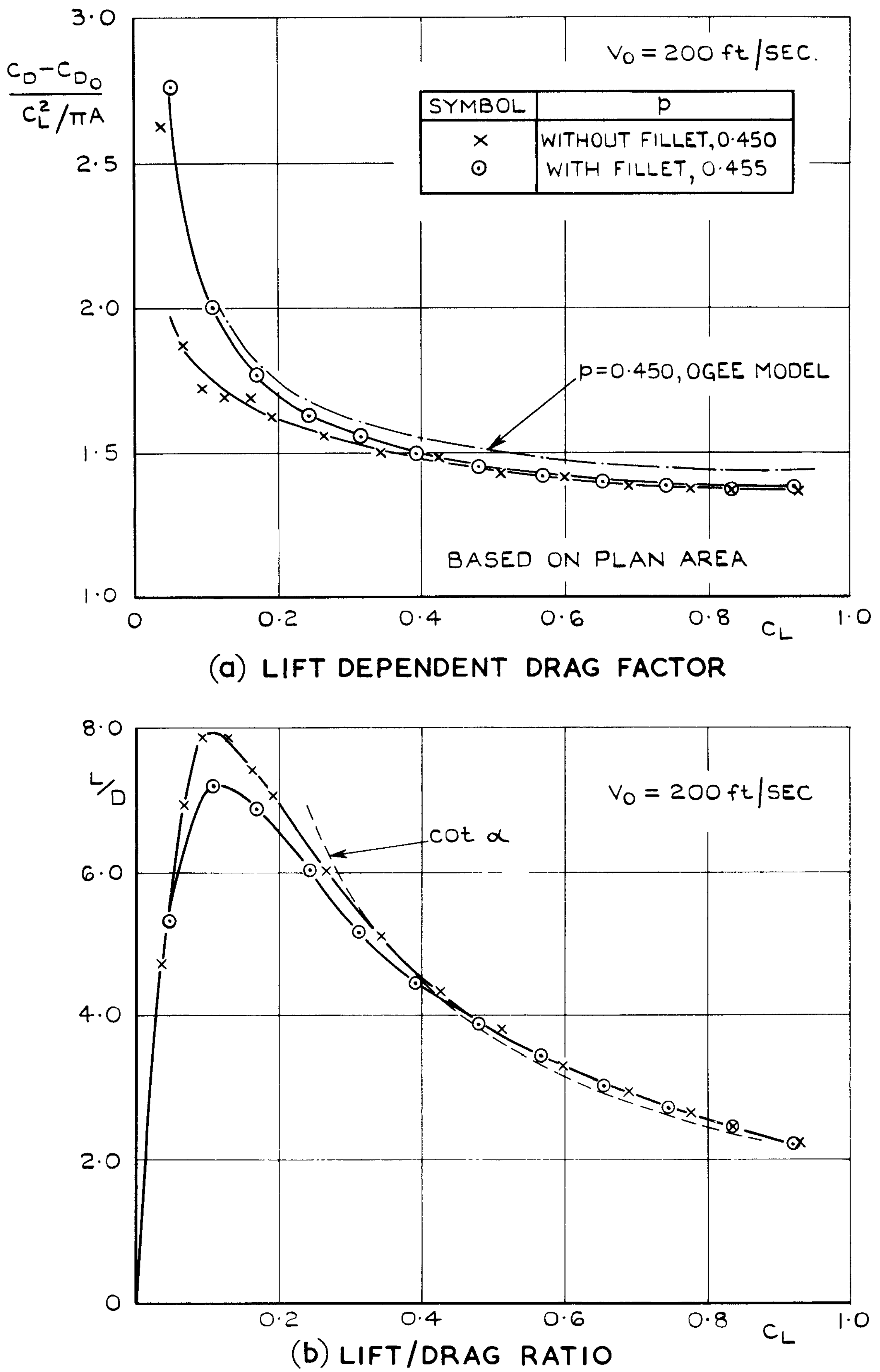

FIG. 10. DRAG CHARACTERISTICS OF THE WING-BODY MODEL WITH AND WITHOUT FILLET, NO NOSE DROOP.

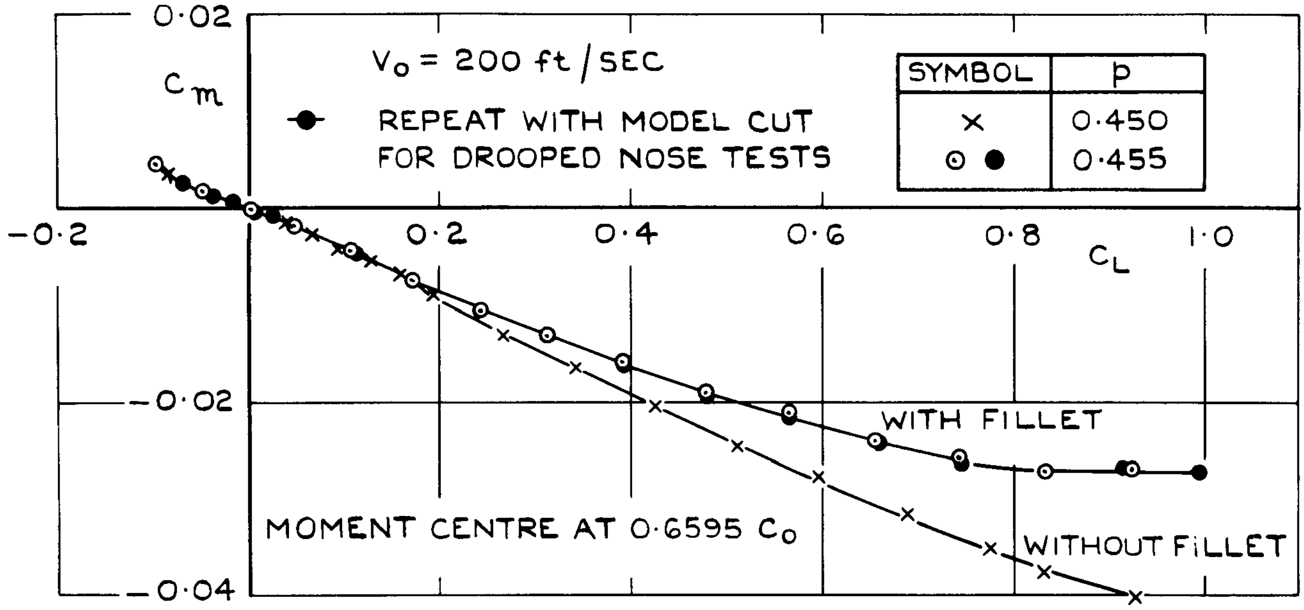

FIG. 11. PITCHING MOMENT COEFFICIENTS, WING-BODY MODELS WITH AND WITHOUT FILLET, NO NOSE DROOP.

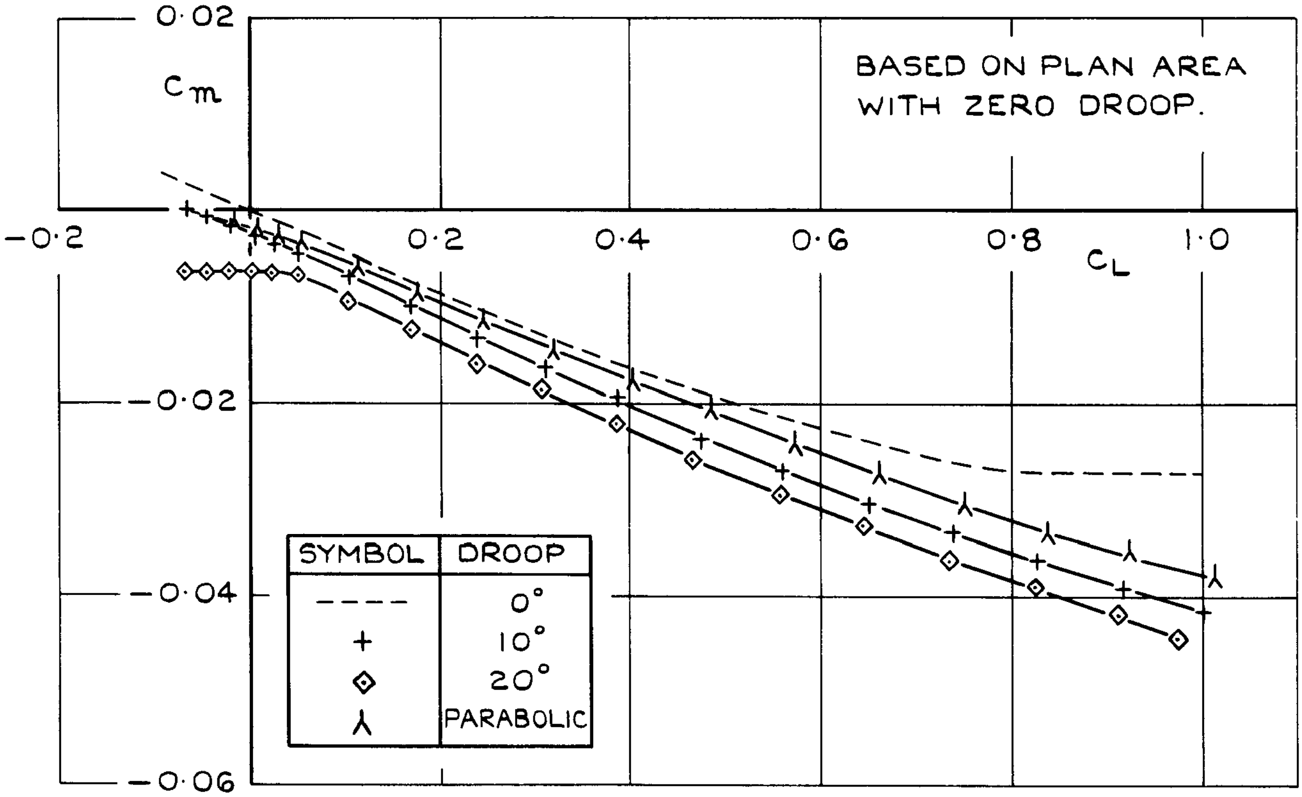

FIG. 12. EFFECT OF NOSE DROOP ON THE PITCHING MOMENTS OF THE WING-BODY MODEL. WITH FILLET.

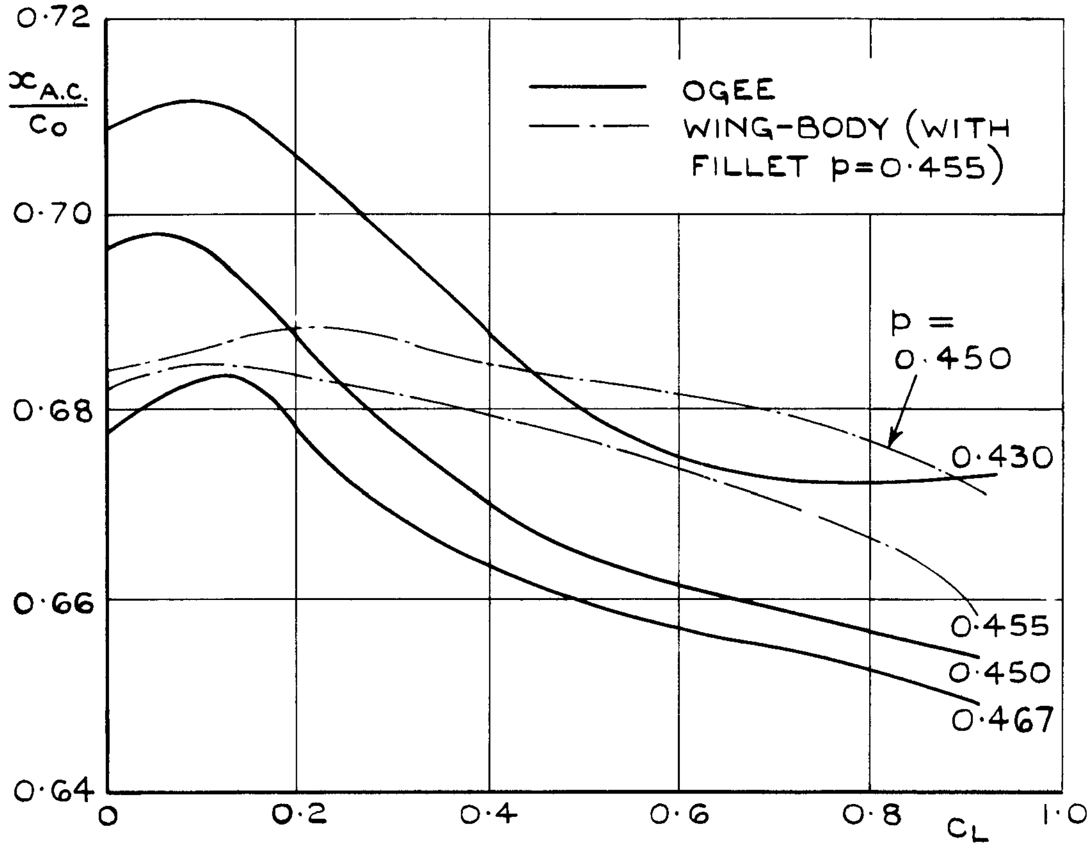

FIG. 13. AERODYNAMIC CENTRE POSITION

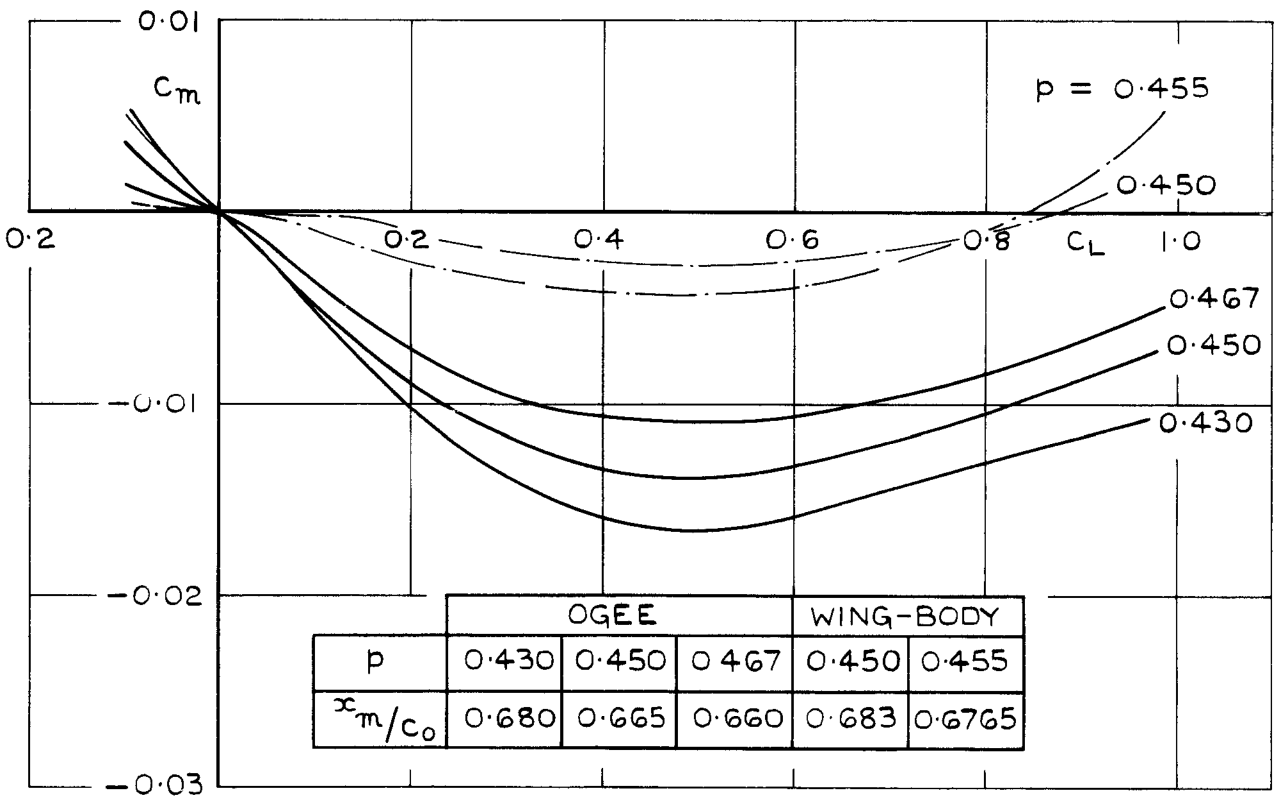

	OGEE			WING-BODY	
p	0·430	0·450	0·467	0·450	0·455
x_m/c_o	0·680	0·665	0·660	0·683	0·6765

FIG. 14. COMPARISON OF PITCHING MOMENT CURVES WITH NEUTRAL STATIC STABILITY AT C_L=0·5

x_m = DISTANCE OF MOMENT CENTRE BEHIND APEX.

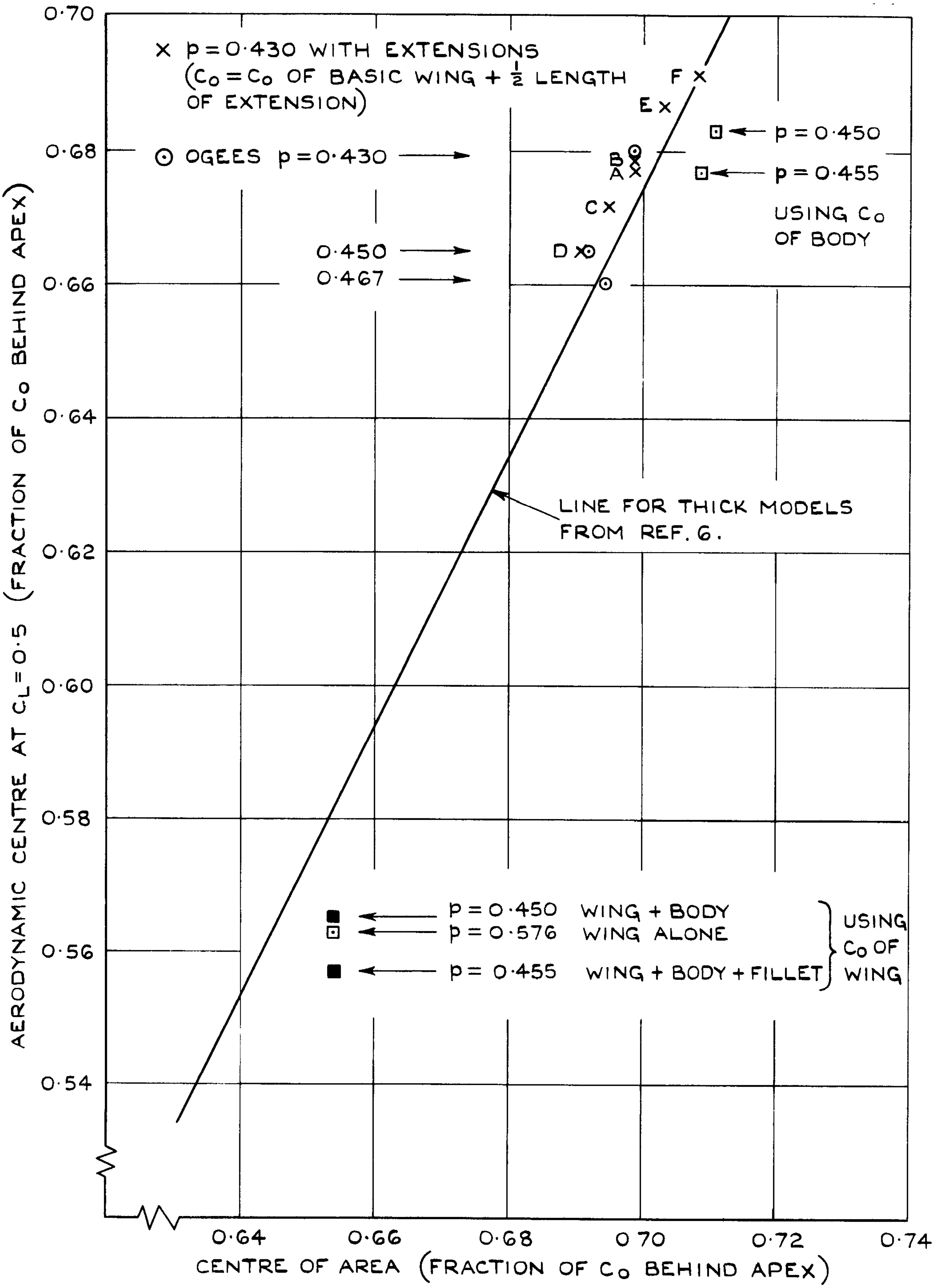

FIG. 15. AERODYNAMIC CENTRE POSITION AT $C_L = 0{\cdot}5$

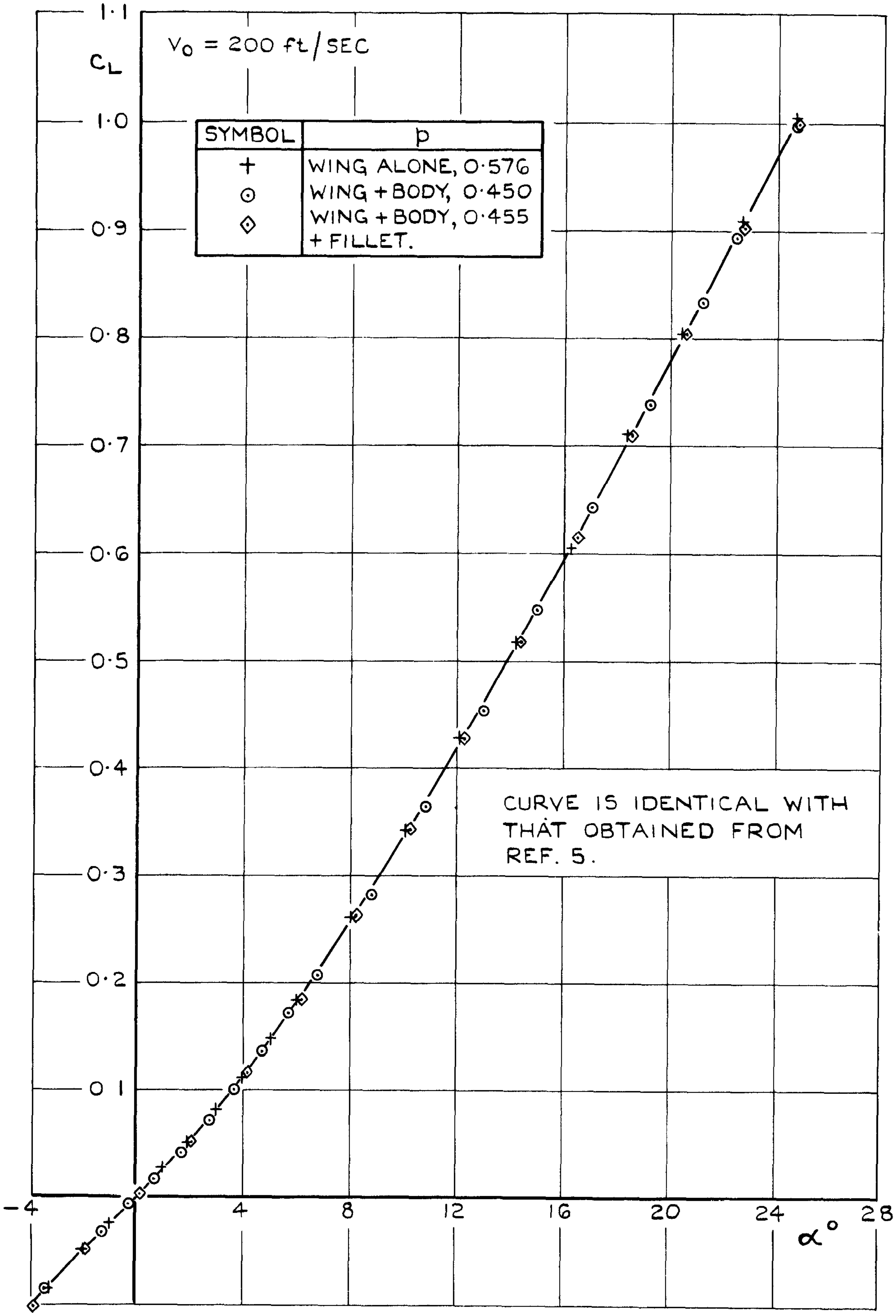

FIG. 16. EFFECT OF BODY AND FILLET ON LIFT COEFFICIENT.
(BASED ON WING DIMENSIONS).

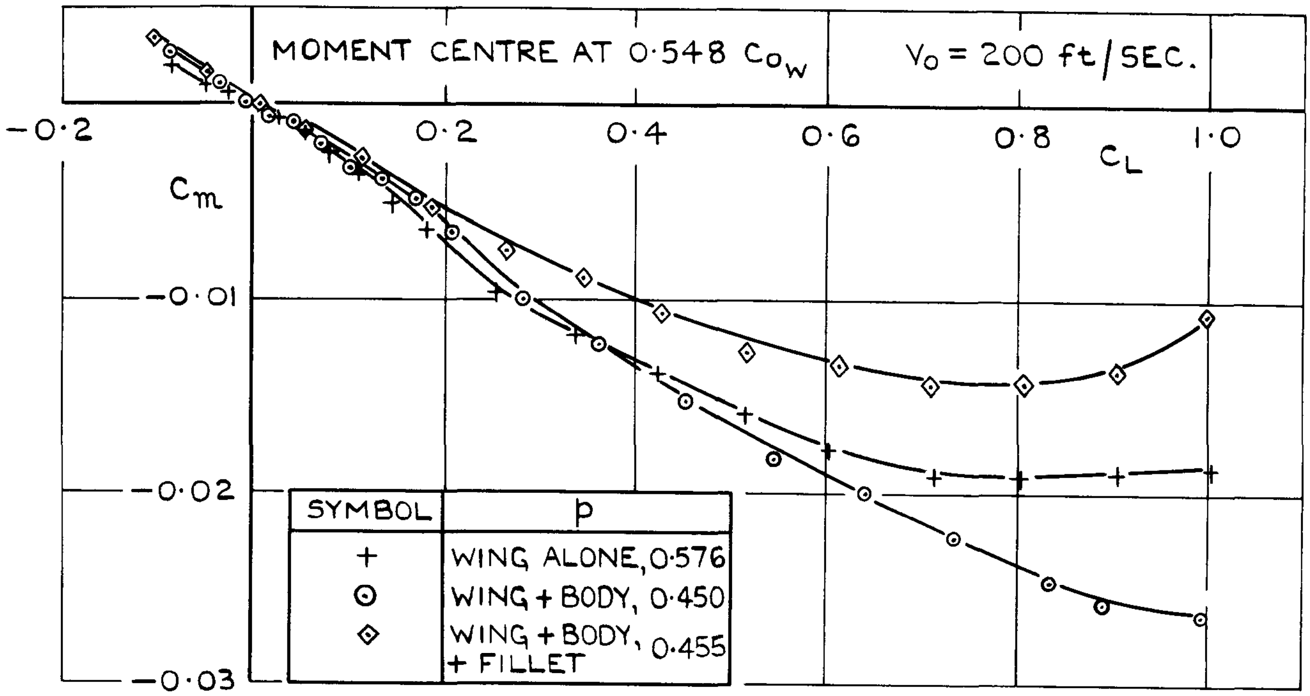

FIG. 17 EFFECT OF BODY AND FILLET ON PITCHING MOMENT COEFFICIENT (BASED ON WING DIMENSIONS).

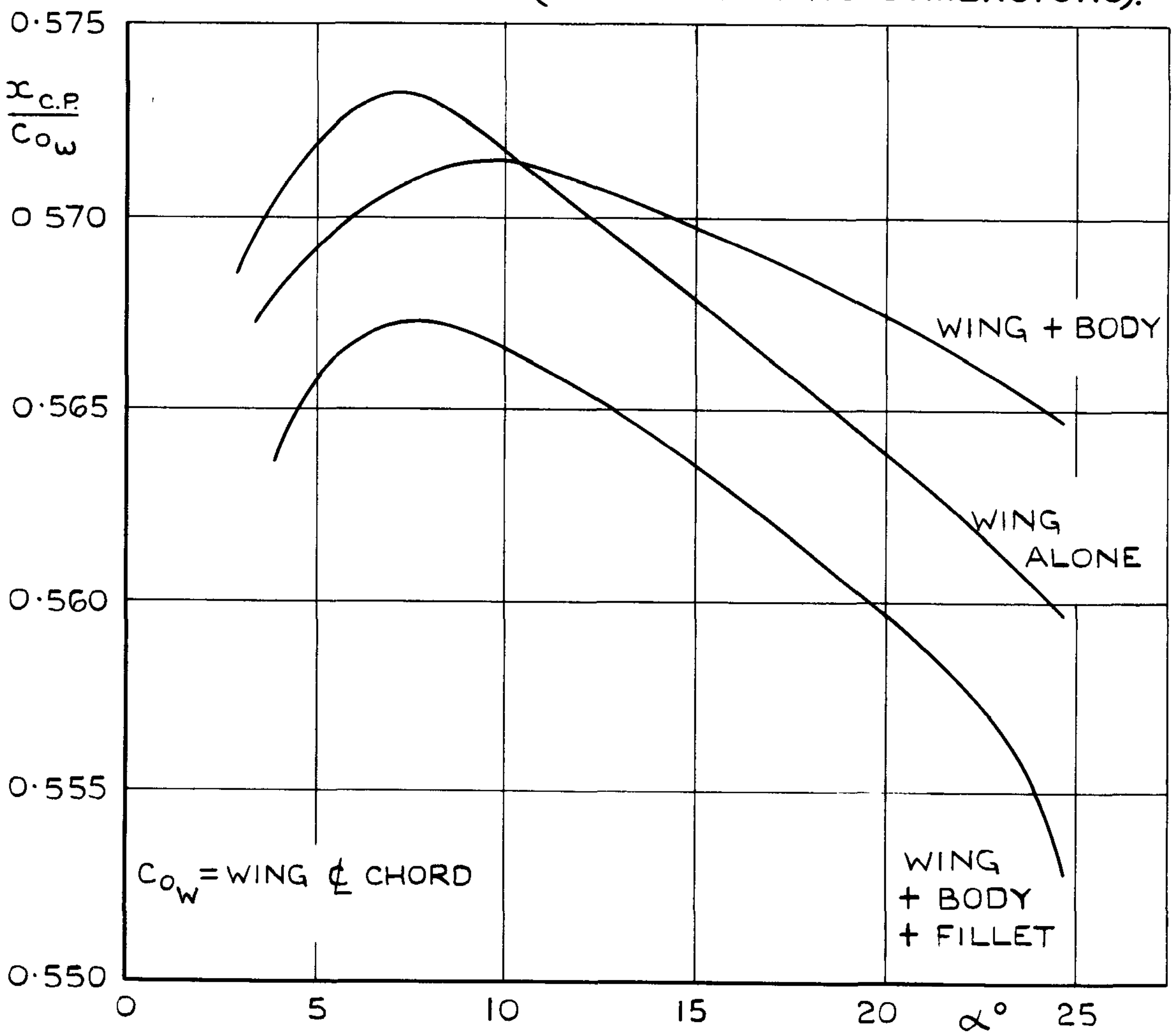

FIG. 18. EFFECT OF BODY AND FILLET ON THE POSITION OF THE CENTRE OF PRESSURE.

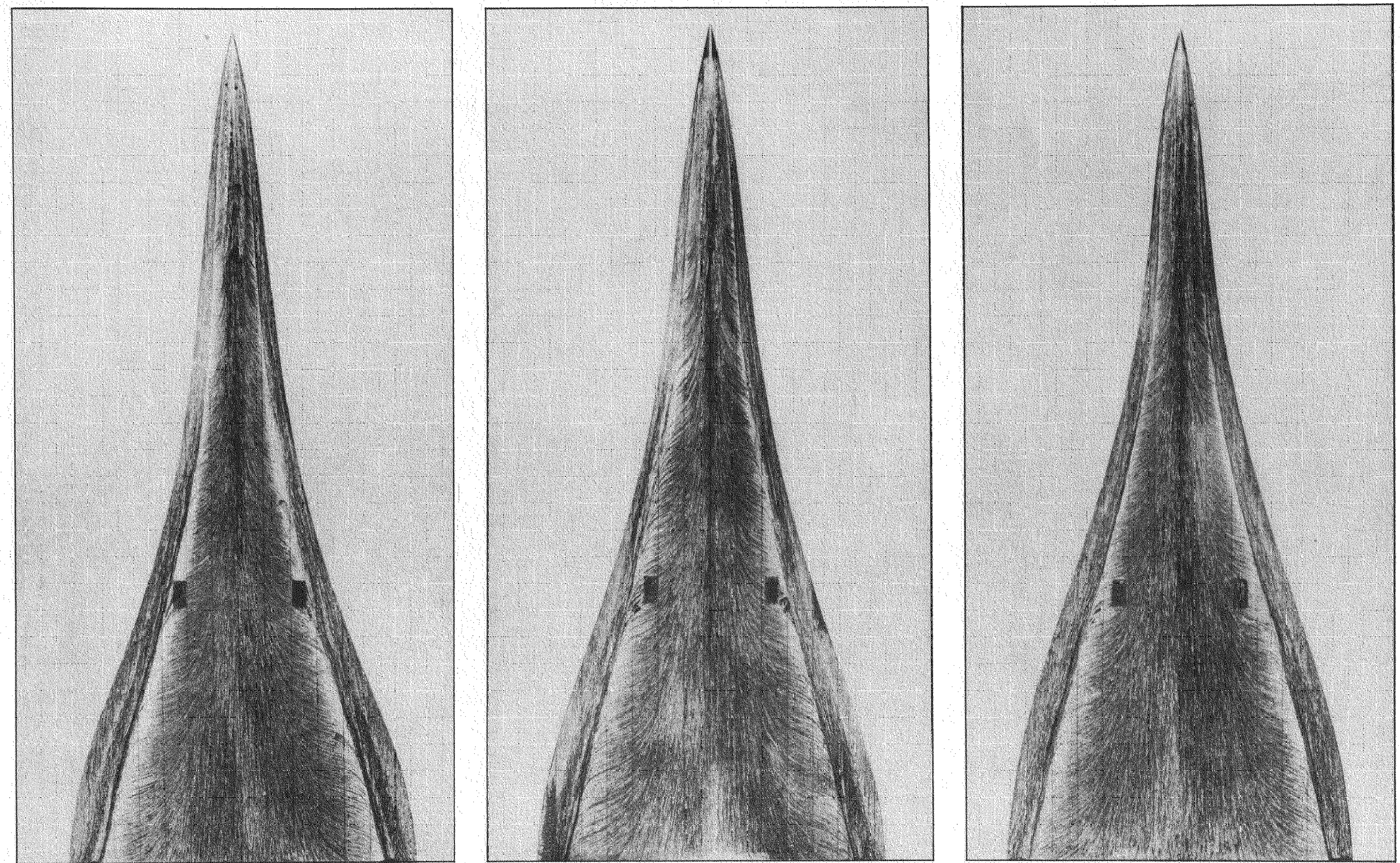

$p = 0{\cdot}430$ $p = 0{\cdot}450$ $p = 0{\cdot}467$

FIG.19. UPPER SURFACE FLOW PATTERNS FOR THE OGEE MODELS
$\alpha = 15^{\circ}$ $V_o = 100$ ft/sec

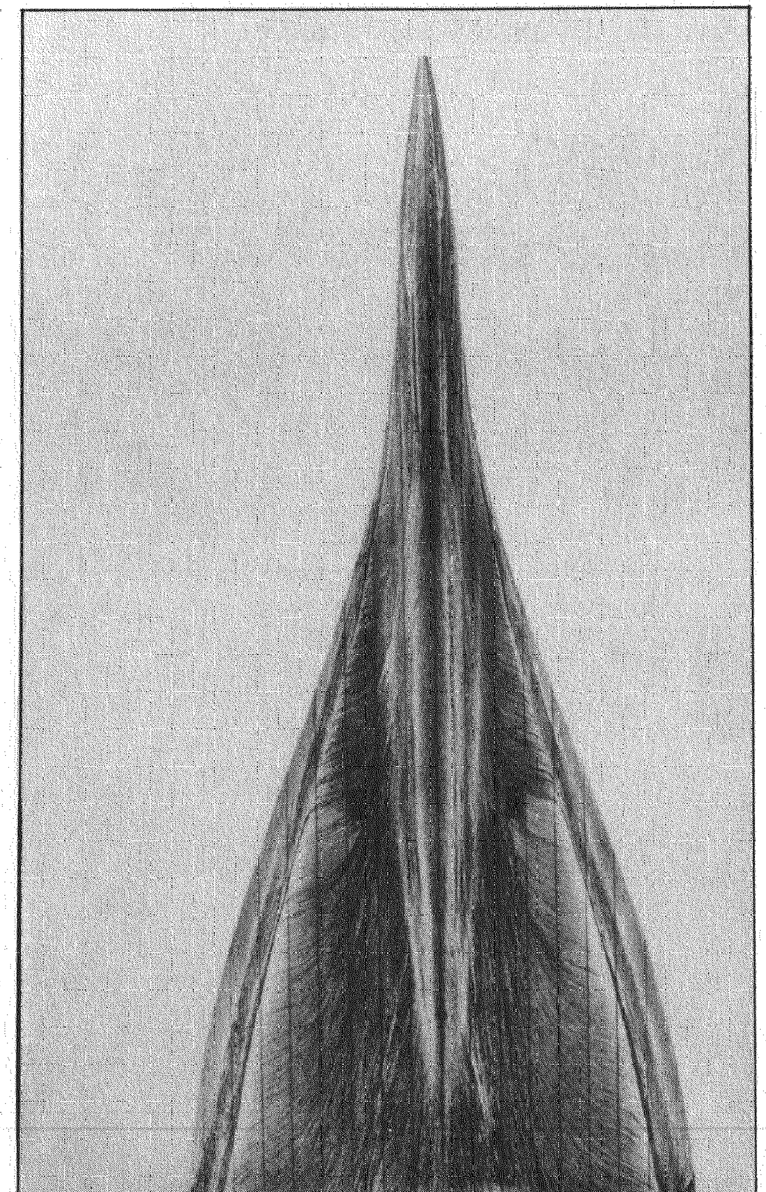

$\alpha = 15°$

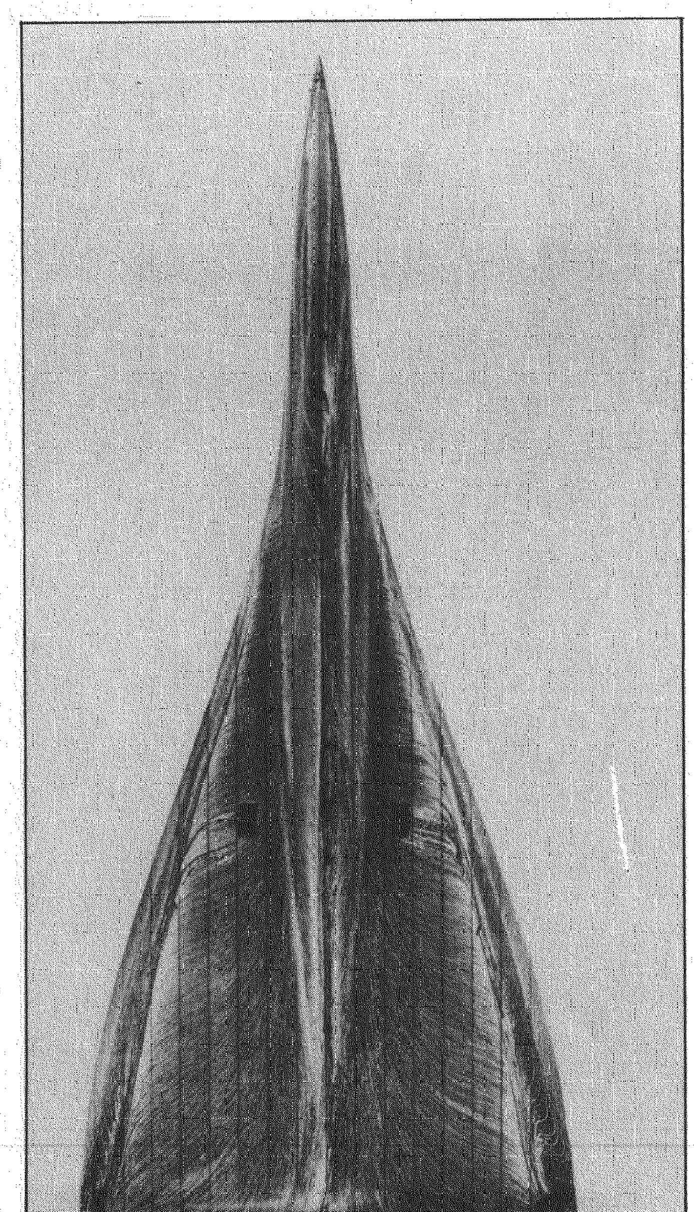

$\alpha = 25°$

FIG.20. UPPER SURFACE FLOW PATTERNS FOR THE WING-BODY MODEL WITH FILLET $V_o = 100$ ft/sec

Printed in England for Her Majesty's Stationery Office by the Royal Aircraft Establishment, Farnborough. Dd.125875. K.4.

A.R.C. CP No.846

533.6.013.13 :
533.6.013.12 :
533.6.013.152 :
533.695.12 :
533.693.4

LOW-SPEED WIND-TUNNEL MEASUREMENTS OF THE LIFT, DRAG AND PITCHING MOMENT ON THREE SYMMETRICAL OGEE-WING MODELS AND ON A SYMMETRICAL SLENDER WING-BODY MODEL. Kirby, D.A. November 1963.

Measurements have been made of the lift, drag and pitching moment of three ogee models and a wing-body model, all having a slenderness ratio (semispan/root chord) of 0.209. The associated surface flow patterns were also observed.

Although the models were symmetrical and did not represent strictly comparable fully optimised designs of possible layouts for a supersonic transport, some useful low-speed aerodynamic comparisons between the integrated or ogee models and the wing-body were obtained. The results show:-

(Over)

A.R.C. CP No.846

533.6.013.13 :
533.6.013.12 :
533.6.013.152 :
533.695.12 :
533.693.4

LOW-SPEED WIND-TUNNEL MEASUREMENTS OF THE LIFT, DRAG AND PITCHING MOMENT ON THREE SYMMETRICAL OGEE-WING MODELS AND ON A SYMMETRICAL SLENDER WING-BODY MODEL. Kirby, D.A. November 1963.

Measurements have been made of the lift, drag and pitching moment of three ogee models and a wing-body model, all having a slenderness ratio (semispan/root chord) of 0.209. The associated surface flow patterns were also observed.

Although the models were symmetrical and did not represent strictly comparable fully optimised designs of possible layouts for a supersonic transport, some useful low-speed aerodynamic comparisons between the integrated or ogee models and the wing-body were obtained. The results show:-

(Over)

DETACHABLE ABSTRACT CARDS

A.R.C. CP No.846

533.6.013.13 :
533.6.013.12 :
533.6.013.152 :
533.695.12 :
533.693.4

LOW-SPEED WIND-TUNNEL MEASUREMENTS OF THE LIFT, DRAG AND PITCHING MOMENT ON THREE SYMMETRICAL OGEE-WING MODELS AND ON A SYMMETRICAL SLENDER WING-BODY MODEL. Kirby, D.A. November 1963.

Measurements have been made of the lift, drag and pitching moment of three ogee models and a wing-body model, all having a slenderness ratio (semispan/root chord) of 0.209. The associated surface flow patterns were also observed.

Although the models were symmetrical and did not represent strictly comparable fully optimised designs of possible layouts for a supersonic transport, some useful low-speed aerodynamic comparisons between the integrated or ogee models and the wing-body were obtained. The results show:-

(Over)

(i) very similar lift characteristics,

(ii) a slightly smaller drag for the wing-body model,

(iii) better static longitudinal stability characteristics for the wing-body model, especially when the wing planform was not faired smoothly into the body.

Attempts to improve the longitudinal stability of one of the ogee wings, by minor planform modifications at the rear of the wing intended to reduce the forward movement of aerodynamic centre with incidence, were largely unsuccessful, but provided some useful data on the effect of trailing-edge shape. For the wing-body model, drooping the nose was a successful modification and it is suggested that a drooped nose version of the wing-body model (without any planform fillet) would have good static longitudinal stability.

(i) very similar lift characteristics,

(ii) a slightly smaller drag for the wing-body model,

(iii) better static longitudinal stability characteristics for the wing-body model, especially when the wing planform was not faired smoothly into the body.

Attempts to improve the longitudinal stability of one of the ogee wings, by minor planform modifications at the rear of the wing intended to reduce the forward movement of aerodynamic centre with incidence, were largely unsuccessful, but provided some useful data on the effect of trailing-edge shape. For the wing-body model, drooping the nose was a successful modification and it is suggested that a drooped nose version of the wing-body model (without any planform fillet) would have good static longitudinal stability.

(i) very similar lift characteristics,

(ii) a slightly smaller drag for the wing-body model,

(iii) better static longitudinal stability characteristics for the wing-body model, especially when the wing planform was not faired smoothly into the body.

Attempts to improve the longitudinal stability of one of the ogee wings, by minor planform modifications at the rear of the wing intended to reduce the forward movement of aerodynamic centre with incidence, were largely unsuccessful, but provided some useful data on the effect of trailing-edge shape. For the wing-body model, drooping the nose was a successful modification and it is suggested that a drooped nose version of the wing-body model (without any planform fillet) would have good static longitudinal stability.

Published by
HER MAJESTY'S STATIONERY OFFICE
To be purchased from
49 High Holborn, London W.C.1
423 Oxford Street, London W.1
13A Castle Street, Edinburgh 2
109 St. Mary Street, Cardiff
Brazennose Street, Manchester 2
50 Fairfax Street, Bristol 1
35 Smallbrook, Ringway, Birmingham 5
80 Chichester Street, Belfast 1
or through any bookseller

C.P. No. 846

S.O. CODE No. 23-9016-46